



University of Stavanger

Faculty of Science and Technology

# MASTER'S THESIS

Study program/ Specialization: MSc Petroleum Geosciences Engineering	Spring semester, 2013  Open / Restricted access
Writer: Tauqeer Ahmed	..... (Writer's signature)
Faculty supervisor:	Karl Audun Lehne (Associate Professor, UIS)
External supervisor(s):	Artur Pryzbylo (Sr. Geophysicist, Edison International)
Title of thesis:  <b>Feasibility report preparation for Cenomanian to Danian age Chalk reservoirs in PL616 through Petro physical and Rock physical analysis using wire line logs.</b>	
Credits (ECTS): 30	
Key words: Petro Physics Rock Physics Geosciences Petroleum Geosciences Engineering Wire Line Log AVO Geophysics & Geology	Pages: .....79.....  + enclosure: .....CD.....  Stavanger, ...14/2013..... Date/year

Front page for master thesis  
Faculty of Science and Technology  
Decision made by the Dean October 30<sup>th</sup> 2009

## **Dedication**

---

Dedicated to my beloved mother, father, my all siblings and my sweet heart (Fiance) for their prayers, support, motivations and fulfilling my all wishes, also dedicated to my teachers who devoted all their efforts to guide me through rocky course of my life, especially to my supervisors for their continuous support and help.

## **Acknowledgments**

---

Praise to Allah, Lord of the worlds, The Beneficent, The Merciful, Who is the entire source of knowledge and wisdom endowed to mankind, who gave me courage and potential to pursue this goal.

It is matter of great pleasure express my sincere regards to my honorable supervisors Mr. Karl Audun Lehne (Associate Professor at University of Stavanger), Artur Przybylo (Sr.Geophysicst Edison International S.P.A) and all others teachers of of MSc Petroleum Geoscience Engineering Department. I am also thankful to Mr. Alejandro Escalona and Mr.Arild Buland for sharing their experience and suggestions through time to time.

I am also extremely thankful to my Parents and siblings for their consistent encouragement, belief in my abilities, their endless love and affection which kept me motivated.

I would like to thank to all my friends and classmates especially to Bereke Kairanov, Simon Nikenyeli, Dora Luz Marin, Luisa Campino, Sveinung Hatløy and Trine Mehus for their sincerity, guidness, help and encouragement.

In the end I will be very thankful to Edison International S.P.A Norway branch for assigning me this project, their guidness, support and I am very thankful to Anne Brit (Data Manager Edison International S.P.A) for her kindness and support. I am especially thankful to University of Stavanger for providing me such a nice platform for my future career.

## **Abstract**

---

PL 616 is a production License located in Southern North Sea of Norwegian territory which was awarded to Edison International S.P.A in APA 2011 round. This area is surrounded by discoveries like Eldfisk, Embla, Valhall and Hod etc.

The elastic properties such as velocity, density, impedance and  $V_p/V_s$  ratio take an important role in reservoir characterization because they are related to the reservoir properties (Xin-Gang & De-Hua Han, 2009). It is helpful to recognize reservoirs on Seismic data because of their different acoustic and shear impedances. Fluid saturated rocks also show variation on seismic with increase of offset (AVO).

The purpose of study is to do petrophysical analysis of surrounding wells to get well understanding about subsurface geology, porosity, saturation, pressure and temperature etc. Rock physical analysis is helpful to predict the shear velocity for brine, oil and gas saturated rocks and to understand elastic parameters relations with velocities and impedance of Cenomanian to Danian chalk reservoirs. Greensberg Castagna (1992) equation is helpful to model shear velocity while Gassman fluid substitution method is good to see the model shear velocity, density and primary velocity trend in case of reservoir saturated with different fluids like water, oil and gas. Synthetic gathers is helpful to observe the effect of fluids on seismic data from zero to far offsets (AVO). Cross plots of Shear and acoustic impedance and velocities are useful to characterize the reservoirs more confidently. Integration of this work is helpful for seismic interpreter to recognize lithology related or fluid related bright spots on seismic sections more confidently.

# Contents

---

Dedication .....	2
Acknowledgments .....	3
Abstract .....	4
Nomenclature .....	11
1 Introduction .....	13
1.1 Introduction .....	13
2 Geology and Stratigraphy .....	14
2.1 Introduction .....	14
2.2 Tectonic History of North Sea .....	15
2.3 Regional Stratigraphy .....	19
3 Methodology and Frame Work .....	23
3.1 Introduction .....	23
3.2 Data .....	23
3.3 Area of Interest .....	25
4 Petro physical Analysis .....	26
4.1 Introduction .....	26
4.2 Quality of logs .....	26
4.3 Zonation .....	28
4.4 Volume of Clay and Sand Estimation .....	31
4.5 Hydrocarbon Corrections .....	32
4.5.1 Methodology .....	32
4.6 Effective Porosity Estimation .....	32
4.6.1 Methodology .....	33
4.7 Effective Water Saturation .....	33
4.7.1 Methodology .....	33
4.8 CPI Plots and Conclusion .....	34
5 Rock physics .....	39
5.1 Introduction .....	39
5.2 Rock physical Analysis .....	39
5.2.1 Methodology and Framework .....	40

5.2.2	Editing Well logs.....	41
5.2.3	Depth vs velocities .....	41
5.2.4	Density vs Velocities.....	44
5.2.5	Vp/Vs versus P-Velocity.....	46
5.2.6	Velocities Comparison .....	47
5.2.7	Vs Prediction .....	49
5.2.8	Vs Calibration .....	50
5.2.9	Gassman Fluid Substitution .....	52
5.2.10	Scenarios & Seismic Gathers .....	55
6	Cross Plots for Reservoir Analysis .....	71
6.1	Introduction .....	71
6.2	Shear versus Acoustic Impedance .....	71
6.3	VpVs versus Acoustic Impedance.....	75
7	Conclusions & Recommendations.....	78
7.1	Conclusions .....	78
7.2	Recommendations .....	78
8	References.....	79

## List of Figures

---

FIGURE 1: SATELLITE IMAGE OF OFFSHORE NORWAY (COURTESY TO GOOGLE EARTH). .....	14
FIGURE 2: CALEDONIAN COLLISION AND RELATED STRUCTURES (EVANS, GRAHAM, ARMUR, & BATHRUST, 2003). .....	15
FIGURE 3: STRUCTURAL REPRESENTATION OF TRIASSIC AGE OF NORTH SEA (EVANS, GRAHAM, ARMUR, & BATHRUST, 2003). .....	17
FIGURE 4: OXFORDIAN TO EARLY KIMMERIDIGIAN STRUCTURAL REPRESENTATION OF NORTH SEA (EVANS, GRAHAM, ARMUR, & BATHRUST, 2003). .....	17
FIGURE 5: L. KIMMERIDIGIAN TO E. CRETACEOUS STRUCTURAL DEVELOPMENT DUE TO MAJOR TECTONIC ACTIVITIES (ATLAS). .....	18
FIGURE 6: PRE DEVONIAN ROCKS IN NORTH SEA OF NORWAY (EVANS, GRAHAM, ARMUR, & BATHRUST, 2003). .....	19
FIGURE 7: MAP VIEW OF PERMIAN SEDIMENTARY BASIN (EVANS, GRAHAM, ARMUR, & BATHRUST, 2003). .....	21
FIGURE 8: MAP VIEW OF PL616 (PURPLE POLYGON) AND SURROUNDING WELLS (RED POLYGONS POINTED BY BLACK ARROWS) USED FOR ACCOMPLISHMENT OF THIS PROJECT (NORWAGIAN PETROLWUM DIRECTORATE). .....	25
FIGURE 9: BOREHOLE DISTURBANCE EFFECTS IN WELL 2/11-9. ....	27
FIGURE 10: BEFORE AND AFTER QC THE LOG DATA (2/11-9). ....	28
FIGURE 11: REPRESENTATION OF TOPS EDITING. RED DOTTED LINE IS TOP OF EKOFISK ON NPD.NO. ....	29
FIGURE 12: TOTAL AND EFFECTIVE POROSITY (GOOLGE). ....	33
FIGURE 13: CPI PLOT OF WELL 2/11-9. ....	36
FIGURE 14: FINAL CPI PLOT OF WELL 2/8-15. ....	37
FIGURE 15: CPI PLOT OF WELL 2/7-23 S. ....	38
FIGURE 16: DEPTH VS PRIMARY VELOCITY BEFORE EDITING. ....	42
FIGURE 17: DEPTH VS P VELOCITY AFTER EDITING. ....	42
FIGURE 18: DEPTH VS SHEAR VELOCITY BEFORE EDITING. ....	43
FIGURE 19: DEPTH VS SHEAR VELOCITY AFTER CORRECTION. ....	44
FIGURE 20: DENSITY VERSUS S- WAVES VELOCITY BEFORE QC. ....	45
FIGURE 21: DENSITY VERSUS S- WAVES VELOCITY BEFORE QC. ....	45

FIGURE 22: VELOCITY RATIO VS PRIMARY VELOCITY BEFORE EDITING. ....46

FIGURE 23: P-VELOCITY VERSUS  $V_p/V_s$  RATIO AFTER EDITING.....47

FIGURE 24: SHEAR VELOCITY VERSUS PRIMARY VELOCITY BEFORE QC.....48

FIGURE 25: SHEAR VELOCITY VS PRIMARY WAVE VELOCITY RELATION AFTER QC.....48

FIGURE 26: MODEL SHEAR WAVES THROUGH GREENSBURG CASTAGNA EQUATION (IN RED). ....50

FIGURE 27: MODEL  $V_s$  AFTER CALIBRATION (IN GREEN).....51

FIGURE 28: CORRELATION BETWEEN MODEL AND MEASURED  $V_s$ . ....52

FIGURE 29: ESTIMATED VALUES OF  $V_p$ ,  $V_s$  AND  $\rho$ . ....54

FIGURE 30: DRY ROCK PLOT OF CHALK INSIDE THE UPPER AND LOWER BOUND AFTER CALIBRATION.  
.....55

FIGURE 31: THREE SCENARIOS OF MODEL  $V_s$  LOGS IN CASE OF OIL (GREEN), GAS (RED) AND WATER  
(BLUE) SATURATION.....56

FIGURE 32: THREE SCENARIOS OF MODEL  $V_p$  LOGS IN CASE OF OIL (GREEN), GAS (RED) AND WATER  
(BLUE) SATURATION.....57

FIGURE 33: DENSITY LOG SCENARIOS IN CASE OF OIL (GREEN), GAS (RED) AND WATER (BLUE)  
SATURATION. ....58

FIGURE 34: THREE DIFFERENT FLUIDS SATURATED FILTER LOGS (WELL 2/7-23 S), OIL (GREEN), GAS  
(RED) AND WATER (BLUE) SATURATION. ....60

FIGURE 35: THREE DIFFERENT FLUIDS SATURATED FILTER LOGS (WELL 2/8-15), OIL (GREEN), GAS  
(RED) AND WATER (BLUE) SATURATION. ....61

FIGURE 36: THREE DIFFERENT FLUIDS SATURATED FILTER LOGS (WELL 2/11-9), OIL (GREEN), GAS  
(RED) AND WATER (BLUE) SATURATION. ....62

FIGURE 37: AI AND SI IN THREE DIFFERENT CASE OF FLUID SATURATION (WELL 2/7-23 S), OIL  
(GREEN), GAS (RED) AND WATER (BLUE) SATURATION. ....63

FIGURE 38: AI AND SI IN THREE DIFFERENT CASE OF FLUID SATURATION (WELL 2/8-15), OIL  
(GREEN), GAS (RED) AND WATER (BLUE) SATURATION. ....64

FIGURE 39: AI AND SI IN THREE DIFFERENT CASE OF FLUID SATURATION (WELL 2/11-9), OIL  
(GREEN), GAS (RED) AND WATER (BLUE) SATURATION. ....66

FIGURE 40: WATER SATURATED AVO EFFECT OF SEISMIC GATHERS (WELL 2/11-9).....68

FIGURE 41: OIL SATURATED AVO EFFECT OF SEISMIC GATHERS (WELL 2/11-9).....69

FIGURE 42: GAS SATURATED AVO EFFECT OF SEISMIC GATHERS (WELL 2/11-9).....70



FIGURE 43: CROSS PLOTS BETWEEN WATER SATURATED AI AND SI FILTERED LOGS COLORED CODED WITH EFFECTIVE POROSITY.....72

FIGURE 44: CROSS PLOTS BETWEEN OIL SATURATED AI AND SI FILTERED LOGS COLOR CODED WITH EFFECTIVE POROSITY.....72

FIGURE 45: CROSS PLOTS BETWEEN GAS SATURATED AI AND SI FILTERED LOGS COLOR CODED WITH EFFECTIVE POROSITY.....73

FIGURE 46: MEASURE ACOUSTIC AND SHEAR IMPEDANCE CROSS PLOT USING WELL 2/8-15.....74

FIGURE 47: MEASURE ACOUSTIC AND SHEAR IMPEDANCE CROSS PLOT USING WELL 2/7-23S.....75

FIGURE 48: VPVS VERSUS AI (ACOUSTIC IMPEDANCE) CROSS PLOT OF WATER SATURATED MODELED LOGS. ....76

FIGURE 49: VPVS VERSUS AI (ACOUSTIC IMPEDANCE) CROSS PLOT OF OIL SATURATED MODELED LOGS. ....77

FIGURE 50: VPVS VERSUS AI (ACOUSTIC IMPEDANCE) CROSS PLOT OF GAS SATURATED MODELED LOGS. ....77

**List of Tables**

---

TABLE 1: PRE-DEVONIAN LITHOLOGY ENCOUNTERED IN NORTH SEA WELLS (EVANS, GRAHAM, ARMUR, & BATHRUST, 2003). .....20

TABLE 2: LIST OF GROUPS AND FORMATION WHICH WERE ENCOUNTERED IN OUR WELLS (NORWAGIAN PETROLWUM DIRECTORATE).....30

TABLE 3: LIST OF WELL TOPS OF GROUPS AND FORMATION IN OUR WELLS (NORWAGIAN PETROLWUM DIRECTORATE). .....31

TABLE 4: LIST OF REGRESSION COEFFICIENTS IN PURE LITHOLOGIES ACCORDING TO GREENSBERG CASTAGNA 1992 (BULAND, OCTOBER 7, 2012). .....49

## **Nomenclature**

---

GR	Gamma Ray
CALI	Caliper Log
NPHI	Neutron porosity Log
RHOB	Bulk Density Log
PHIE	Effective Porosity
SWE	Effective Water Saturation Log
RT	Resistivity Log
PHID	Porosity through density
Amp	Amphibolites
Gab	Gabbro
Gns	Gneiss
Grt	Granite
Sch	Schist
Mag	Magmetite
Qzt	Quartzite
AVO	Amplitude versus offset
RPM	Rock physical model
Vs	Shear Velocity
Vp	Primary Velocity
DT	Sonic Log
DTS	Shear Sonic Log
IP	Interactive Petrophysics
PL	Production license
QC	Quality Check
Gp	Group
Fm	Formation
SST	Sandstone
Vcl	Volume of Clay
NPHIC	Neutron Porosity Correction

NPHIcl	Neutron porosity of Clay
$\phi$	Porosity
a	Lithology factor
m	Cementation factor
n	Saturation factors

# 1 Introduction

## 1.1 Introduction

Edison International Norway Branch is an exploration company which has operational rights for PL 616. It is a production license in a Southern North Sea of Norwegian territory. The objective of this project was to prepare feasibility report for this license using the wire line data of surrounding wells. The work which will be adopted for this project is summarize in list below

- Petrophysical studies
- Rock physical analysis
- Modeling shear velocity
- Generated Fluid substitution models
- Seismic gathers and AVO effect.

The motivation behind this project was to develop the accurate relation between rock properties and seismic attributes to reach the target more confidently through Petrophysical and Rock physical analysis. Well logs are the direct way to know about subsurface therefore Petrophysical analysis will help to understand about subsurface lithologies, porosities, saturation,  $V_{clay}$ ,  $V_{sand}$ ,  $V_{chalk}$ , temperature and pressure. On the petro physical basis we will be able to select the area of interest for Rock physical model. Elastic properties such as velocities, impedance, density and velocity ratios are important to understand because they have great influence on reservoir characterizations (Xin-Gang & De-Hua Han, 2009). Integration of rock physical models with well logs, core data, geological models and seismic data can play effective role in delineating the lithology and fluid content for the future well (Xin-Gang & De-Hua Han, 2009). In this project shear velocity will be model by using Greensberg Castagna equation. Further Gassman fluid substitution will help us to see the effect of model shear velocity, primary velocity and density in case of Water, Oil and Gas saturation (Buland, October 7, 2012). Seismic gathers will be used to see the effect of pore fluids on the seismic traces from to zero to far offset. All well data and softwares (IP & Rock Doc) were provided by Edison International and University of Stavanger.

## 2 Geology and Stratigraphy

### 2.1 Introduction

Due to increase in demand of oil and gas in market, exploration companies are interested in exploring more and more reservoirs. Previous exploration work in offshore of Norway reveals that there is lot of potential there. Besides exploring shallow reservoirs, companies are looking for deep reservoirs also. To achieve the targets more confidently we need to develop well understanding about the geology of the area because Norwegian offshore has very complex geological history. Offshore Norway is divided into three parts named as Barents Sea, Norwegian Sea and North Sea (Figure 1).

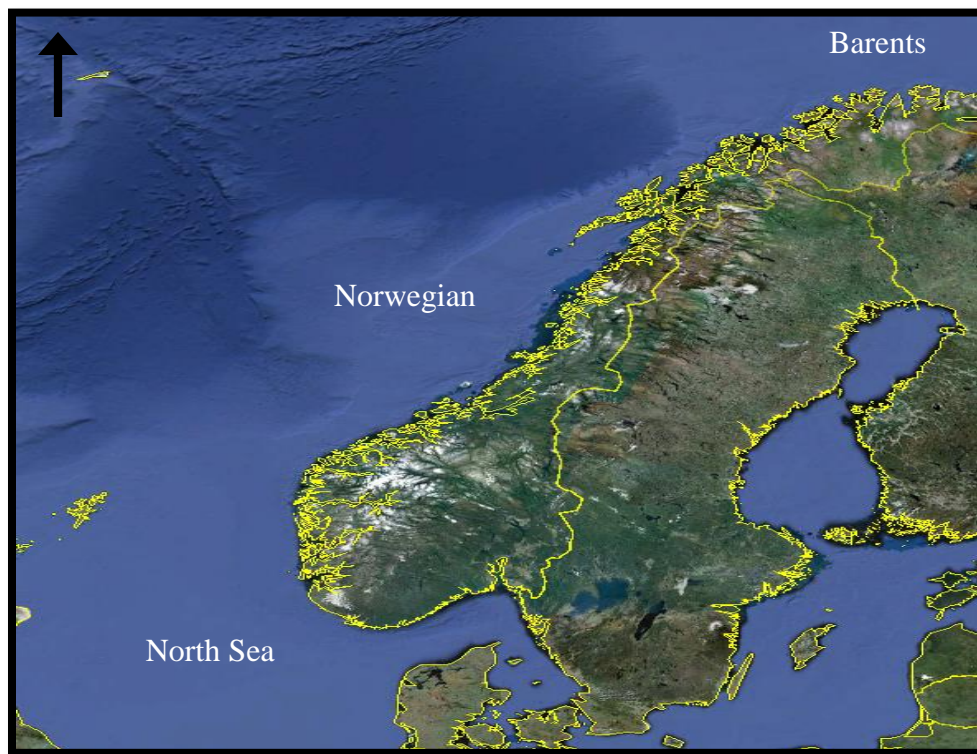


Figure 1: Satellite image of Offshore Norway (Courtesy to google earth).

## 2.2 Tectonic History of North Sea

The paleo tectonic events are very important in development of current picture of North Sea basin specially.

- Caledonian Event.
- Hercynian Event.
- Rifting and Post Rifting Events.
- Intracratonic Events.

Effects of these tectonic events has been influence the development of positions and directions of geological basins which leads into the classification of North Sea into two sub sedimentary basins called Southern North Sea and Northern/Central North Sea Basin.

Collision between North American – Greenland Plate with NW-European plate along Scottish-Norwegian and Appalachian forebelts was the result of Caledonian orogeny and narrowing of Iapetus Ocean (Figure 2).

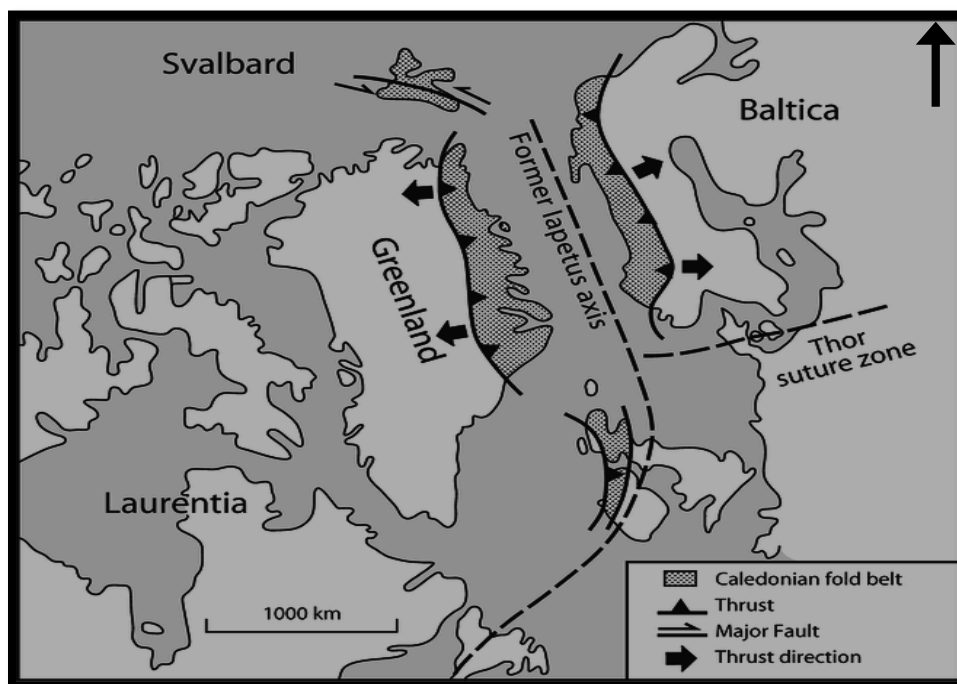


Figure 2: Caledonian collision and related structures (Evans, Graham, Armur, & Bathrust, 2003).

Hercynian phase was the major uplift which formed the southern margin of North Sea. This orogeny was result of narrowing and closure of North Sea basin (Evans, Graham, Armur, & Bathrust, 2003).

In the end of Hercynian orogeny (Permian) the compressional forces stopped and southern mountain chains consolidated with craton to north of North Sea basin. New extensional features develop with formation of two Intracratonic basins which were separated by W-E trending Highs. Salt tectonics (Zechstein) played great influence on sedimentation pattern and development of high pressure reservoirs (Evans, Graham, Armur, & Bathrust, 2003).

In Triassic age new events like subsidence and rifting was cause of development of Viking Graben, cause of uplifting and erosion of high areas. Salt deformation and major uplifting had great impact and importance in development of North Sea basin specially exploration point of view. Major tectonics event in the North Sea basin was caused by major rifting in Atlantic Ocean and in associated areas which affected the crustal stability, adjacent areas and pattern of sedimentation. During the Callovian subsidence and uplifting was responsible for the sediment (locally) supply by developing the deep hole in Viking and Central Grabens mean while salt deformation was very intensive and responsible for sediment control in Southern North Sea Basin. Below figures 3 to 5 are well illustration of structural map of North Sea which developed from tertiary to Early Cretaceous ages (Evans, Graham, Armur, & Bathrust, 2003).



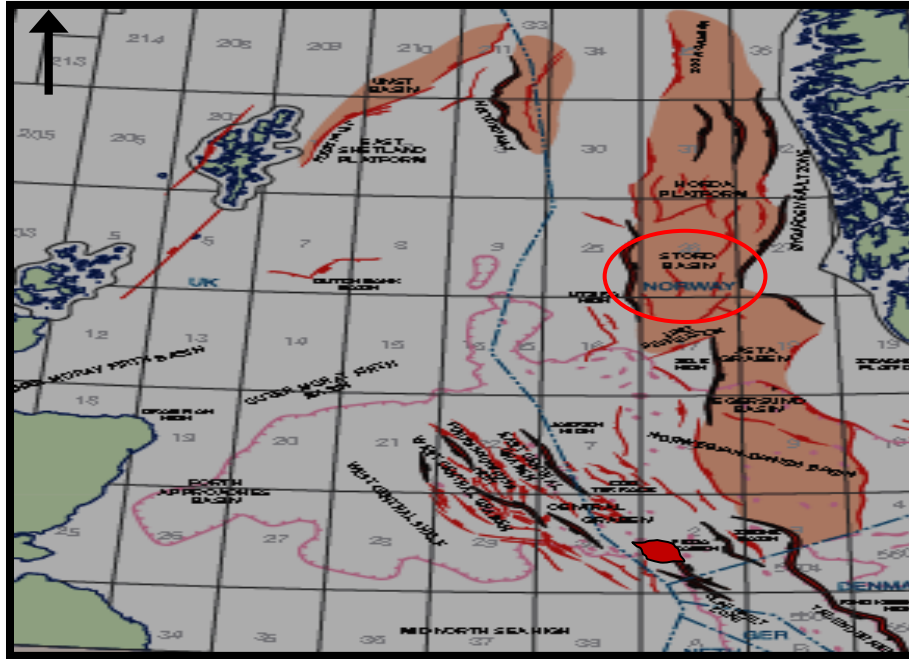


Figure 3: Structural representation of Triassic age of North Sea (Evans, Graham, Armur, & Bathrust, 2003).

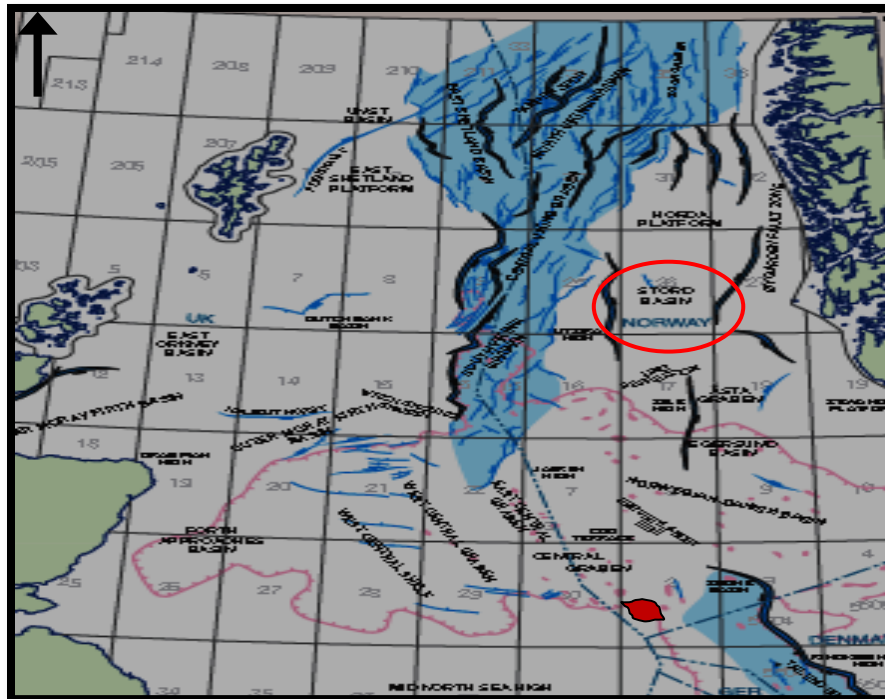


Figure 4: Oxfordian to Early Kimmeridgian structural representation of North Sea (Evans, Graham, Armur, & Bathrust, 2003).

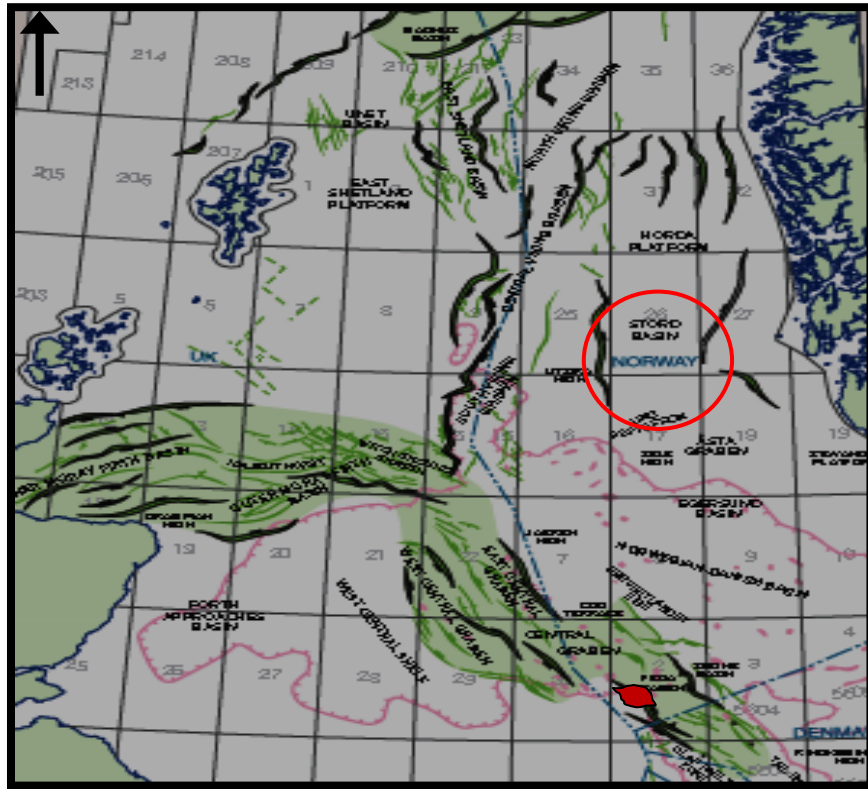


Figure 5: L. Kimmeridgian to E. Cretaceous structural development due to major tectonic activities (Evans, Graham, Armur, & Bathrust, 2003).

Cretaceous was end of tectonic activities and covering of basin with shallow sea was happened. This was the cause of the depositional conditions for carbonate specially chalk and limestone etc. Early tertiary was another phase of tectonic activity which was cause of uplifting and erosion of chalk from high blocks. This all was due to Atlantic rifting and unconformable surfaces like BCU developed at this time. These events have importance for exploration point of view because huge oil deposits like Ekofisk formed this time. Atlantic rifting was the cause of SE movement of European plate which demolished in the middle of tertiary but subsidence was continuous during that time. Volcanic sediments presence in the basin is prove of intensive volcanic paleo event (Evans, Graham, Armur, & Bathrust, 2003).

Continuous sediment supply made the room for thick tertiary sediment to deposit towards basin wards. This process was result of formation of big reservoirs in North Sea of tertiary age for examples Frigg, Gannet and Petrel etc (Evans, Graham, Armur, & Bathrust, 2003).



granitic intrusion were recorded during Late Silurian to Early and or Mid Devonian ages. There is some Pre-Devonian Lithology identification from different wells of Norwegian offshore territory (Table 1).

Table 1: Pre-Devonian Lithology encountered in North Sea wells (Evans, Graham, Armur, & Bathrust, 2003).

<b>Wells</b>	<b>Lithologies</b>	<b>Age</b>
<b>3/7-1</b>	High grade Gneiss & Green schist	Middle Llandovery to Lower Devonian
<b>8/3-1</b>	Biotite Schist	Lower to Middle Pridoli
<b>10/5-1</b>	Granite	Upper Proterozoic
<b>16/2-1</b>	Biotite Micro granite	Upper Ordovician to Lower Devonian
<b>16/6-1</b>	Mica Schist	Lower to Upper Ordovician
<b>25/11-1</b>	Gneiss, Marble and Schist	Upper Ordovician

There is Old Red Sandstones deposition with some local unconformities of Devonian age in some parts of offshore North Sea which developed because of erosion and locally uplifting of foot wall. These were occurred at different sets of time which lead to classification of Old Red Sandstone into Lower, Middle and Upper Old Red Sandstone categories. Sand stones and conglomerates deposits were encountered in some wells (Evans, Graham, Armur, & Bathrust, 2003).

The marine continental transitions lead to deposition of Limestone, evaporites and chalk in Mid Devonian age. Devonian marine incursions are reported from the Orcadian Basin, Occurring with an orbital cyclicity and might be correlated to high stand sea level (Evans, Graham, Armur, & Bathrust, 2003).

Sandstone, shale and coal sequences of Carboniferous age were encountered in some wells of North Sea especially in UK part. Wells drilled in offshore of Norwegian North Sea also proved the presence of Limestone, millstone grit and sandstone of carboniferous age. Variety of the Carboniferous sediments represent marine, fluvial, deltaic and continental environment of deposition (Evans, Graham, Armur, & Bathrust, 2003).

Rock sequences of Permian age in North Sea is termed as Rotilegend and Zechstien Group which comprise of sandstones with some basal volcanics (Rotligned Group) while upper sequence (Zechstein Group) comprises of carbonates, evaporites and clastic rocks. Sandstone of Rotilegend

Group were deposited in eolian environment is of poor reservoir quality and they deposited over Ringkøbing Fyn High and Mid North Sea High. Volcanic intrusion caused by the active rifting at that time could be the cause of destruction of quality of reservoir (Evans, Graham, Armur, & Bathrust, 2003). Zechstien sediments are missing from some part of North sea but they encountered in some wells like well 2/7-23 S.

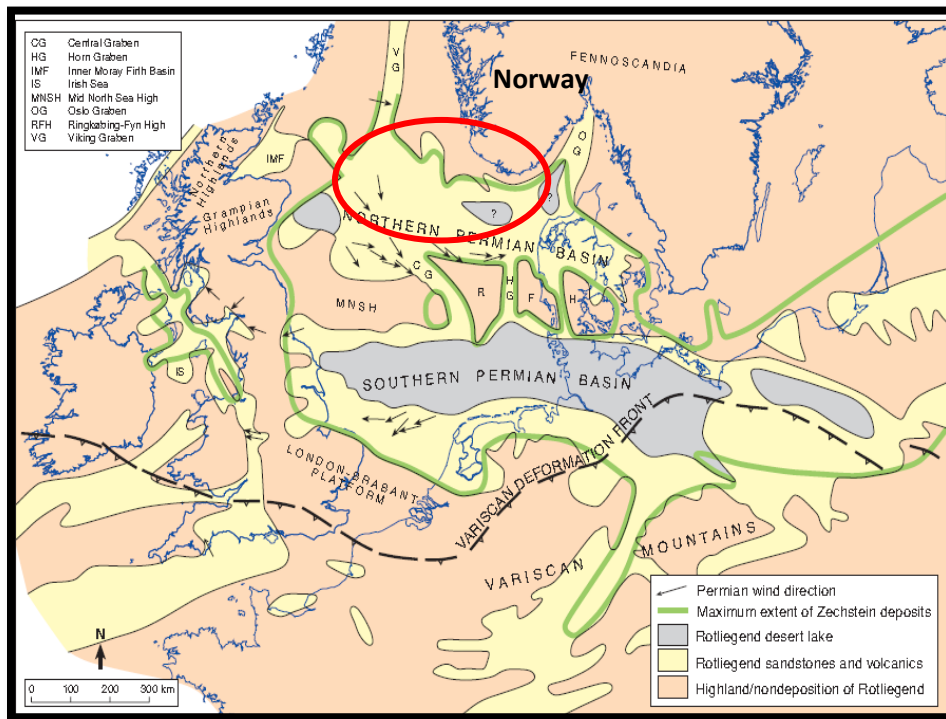


Figure 7: Map view of Permian sedimentary basin (Evans, Graham, Armur, & Bathrust, 2003).

Triassic period start from 251.4 Ma and ends 199 Ma ago according to Jin-Yugan et al and Palfy et al., 1997 and 2000 respectively (Evans, Graham, Armur, & Bathrust, 2003). Regional tectonics had great control over deposition of Triassic sequences that why sequence of Northern North Sea less thickness than the sequences of Southern North Sea with some internal unconformities. Triassic sequences were encountered in some wells which comprises of shale, mudstones, conglomerates, sandstones and siltstones of Smith Bank Formation and Skagerrak Formation which deposited in alluvial and fluvial environment. Uplifting of Fennoscandian Shield lead to deposition of fine grain Clastic deposits named as Skagerrak Formation (Evans, Graham, Armur, & Bathrust, 2003).

Phase of thermal subsidence following Permo Triassic rifting lead to deposition of Early Jurassic marine deposits. Sub aerial dome formation and development of plume lead to the deposition of paralic sediments of Middle Jurassic age in North Sea. Late Jurassic period was the time of intensive rifting which leads to formation of major extensional structures. Rotation of fault blocks lead to deposition of shale in structural lows which preserved during cretaceous erosional event. Jurassic sandstone was encountered in some wells of UK and Norwegian North Sea sectors and it is believed that this was deposited from distal towards the delta (Evans, Graham, Armur, & Bathrust, 2003).

## 3 Methodology and Frame Work

### 3.1 Introduction

The approach which was adopted for the accomplishment of this project actually consists of two parts;

- Petro physical Analysis.
- Rock physical Analysis.

Interactive petro physical (IP) software will be used for the Petro physics part. After selection of suitable wells first and important step will be to check the quality of data and then start the petro physical analysis of the wells. After The QC of all logs, methods and techniques which were adopted for petro physical part are listed below;

- Zoning and Lithology estimation.
- Vcl calculation.
- Hydrocarbon Correction in Reservoir zones.
- Estimating effective porosity.
- Calculation of Effective water Saturation.

For quantitative analysis of reservoir rock physical approach was adopted. The basic work flow of this part is mention below;

- QC the Logs Using Rokdoc software.
- Prediction of Vs.
- Apply fluid substitution to replace hydrocarbons with in all brine intervals.
- Elastic parameters were used to provide the quantitative information about reservoir.
- AVO analysis was used for qualitative information and to avoid the misinterpretation about the target.

### 3.2 Data

Wells which were selected for the master thesis task are listed below

1. 2/7-23 S
2. 2/8-15

### 3. 2/11-9

Well 2/7-23 S was drilled in Embla field which is an Oil field (Figure 8). Total depth of this well was 4760 meter and it was penetrated into Devonian age rocks. Oil shows were encountered in Nordland Group, Hordland Group, Shetland group, Ekofisk and Tor Formations. Prove reservoir in this area was chalk of Ekofisk, Tor and Hod Formation.

Well 2/8-15 was drilled to Northeast of Valhall field to test the potential of Noekken field (Figure 8). The main reservoir sections in this area were Tor and Ekofisk formations of Cretaceous age. Late cretaceous age (HOD Formation) was the oldest penetration age of this well with total depth of 3750 meters. Well was ended as dry because no oil shows were found.

Well 2/11-9 was drilled in south of HOD field with in PL033 (Figure 8). This license include Valhall and Hod. Early carboniferous was the oldest penetration age of this well with total depth of 4406 meters. Oil shows were observed in Ekofisk, Tor and Hod formation but reservoir was not of good quality. There was no Oil show in sandstones of Carboniferous age. The well was abandoned as dry with some Oil shows in it (Norwegian Petroleum Directorate).

Gamma Ray, Density, Neutron, Resistivity, Shear Sonic Log and Sonic Log were run in these wells which were important for Rock and Petro physical analysis. The quality of logs was much better as compare to other well near to PL 616.



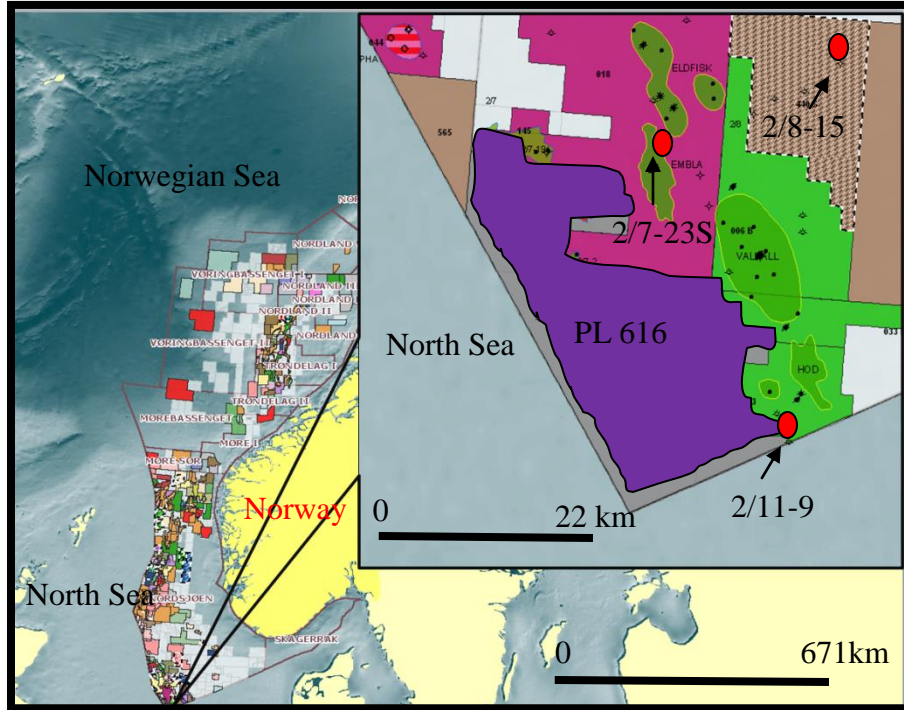


Figure 8: Map view of PL616 (purple polygon) and surrounding wells (red polygons pointed by black arrows) used for accomplishment of this project (Norwegian Petroleum Directorate).

### 3.3 Area of Interest

After detail review of the well logs information it was concluded that Cenomanian to Danian Chalk of Ekofisk, Tor, Hod and Hidra can be good for Rock physical modeling. Hidra was not encountered in well 2/8-15 because it was short in depth of penetration as compare of rest of wells. This decision was made because these were the common lithologies in our three wells.

## 4 Petro physical Analysis

### 4.1 Introduction

The Petrophysical evaluation was done by using three wells from Southern North Sea named 2/7-23 S, 2/8-15 and 2/11-9. Logs which were used are listed below.

- Caliper (CALI) Log
- Gamma Ray (GR) Log
- Neutron Porosity (NPHI) Log
- Density (RHOB) Log
- Sonic (DT) Log
- Shear Sonic (DTS) Log
- Resistivity (RT) Log

### 4.2 Quality of logs

The quality of wells was not good so the first important thing which was done to QC that logs of all wells. Logs data of the wells which were affected by bore hole diameter disturbance (Red polygons in Figure 9) and wash out factors especially well 2/11-9 was much effect specially in Chalk reservoir sections of Ekofisk, Hod and Tor Formations. Figure 9 below is well representing of washout disturbance in well which may lead to wrong path. These factors can be easily recognized on Caliper logs. These factors also effects on RHOB, NPHI, Shear Sonic and Sonic Logs. Ekofisk, Tor and Hod are formations have Chalk Lithology but here gamma ray is show very high values which is wrong so while calculating volume of clay we took care of this factor and QC the log by using different techniques (Figure 9-10). These factors can be cause of wrong interpretation about reservoirs properties like porosity and Hydrocarbon Saturation.

The logs which were mostly affected by the environmental factors and edited were sonic log and shear sonic log.

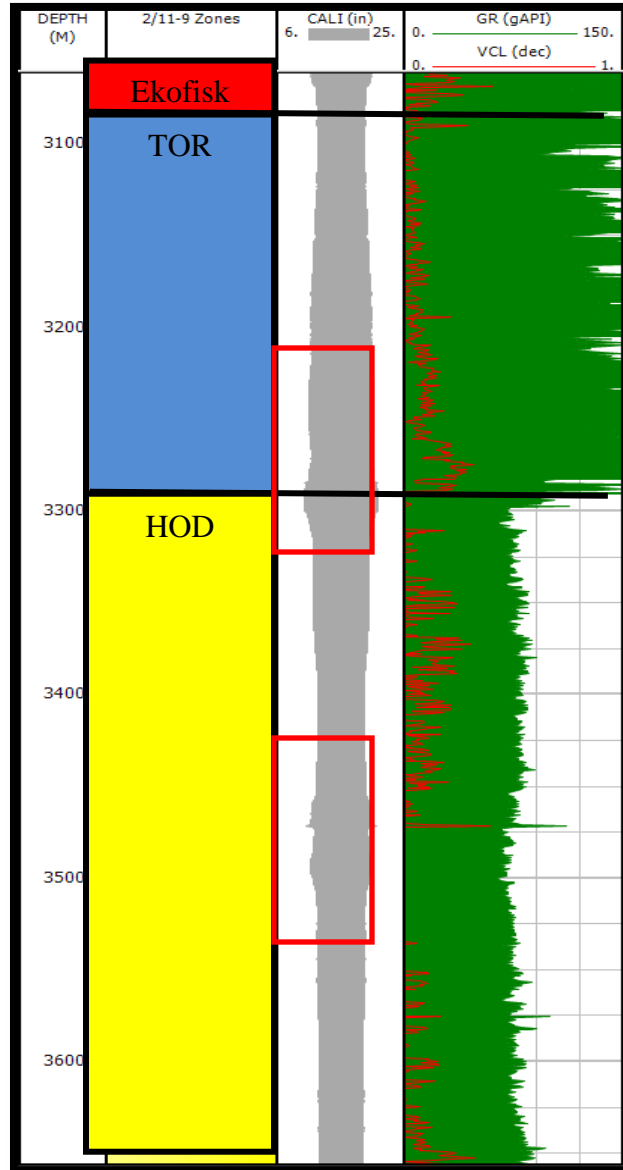


Figure 9: Borehole disturbance effects in Well 2/11-9.

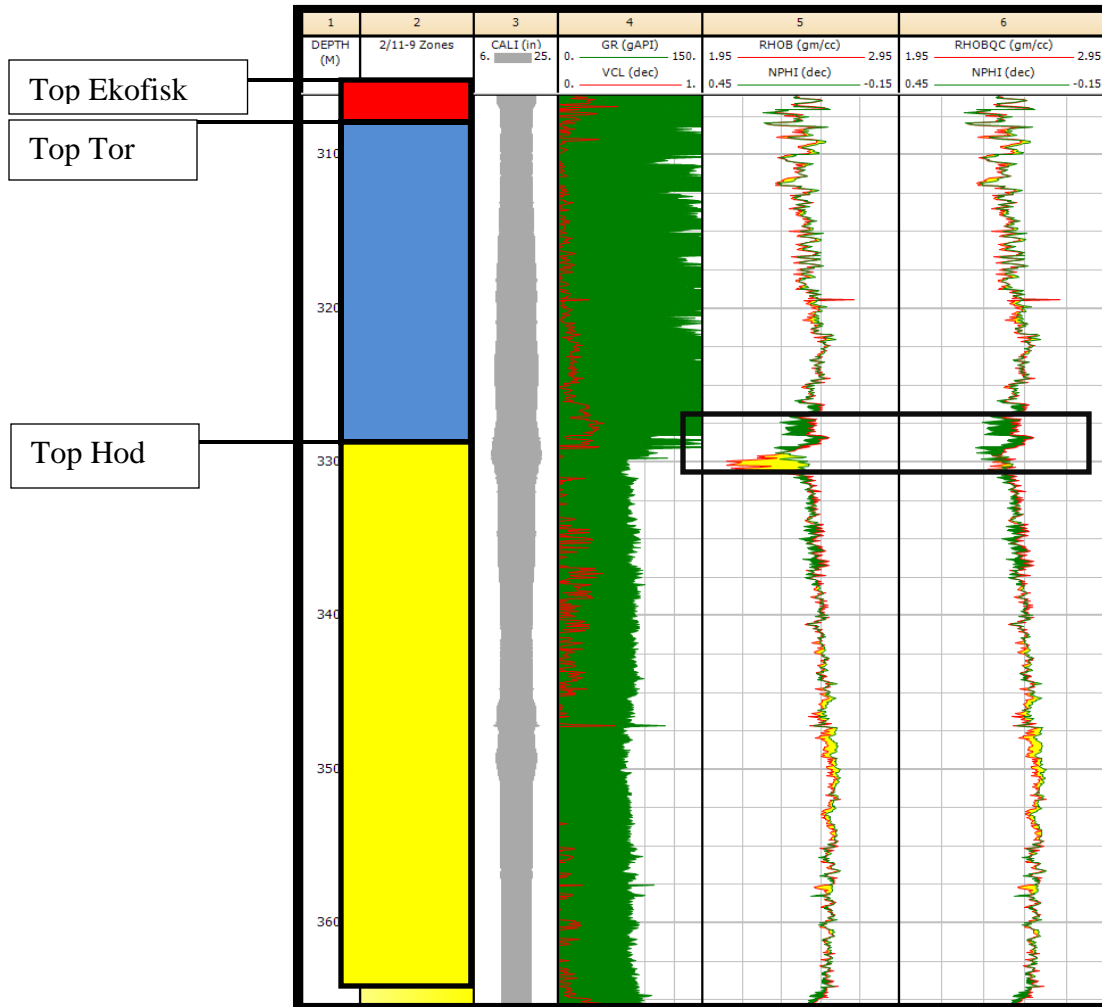


Figure 10: Before and After QC the log data (2/11-9).

### 4.3 Zonation

Zones were defined by using well tops information from official website of Norwegian Petroleum Directorate. These tops data was confirmed by correlating them with Gamma Ray, regional stratigraphy and previous Petrophysical work which gave confident to edit some zone where there was doubt especially in Ekofisk zone of well 2/7-23 S (Figure 11).

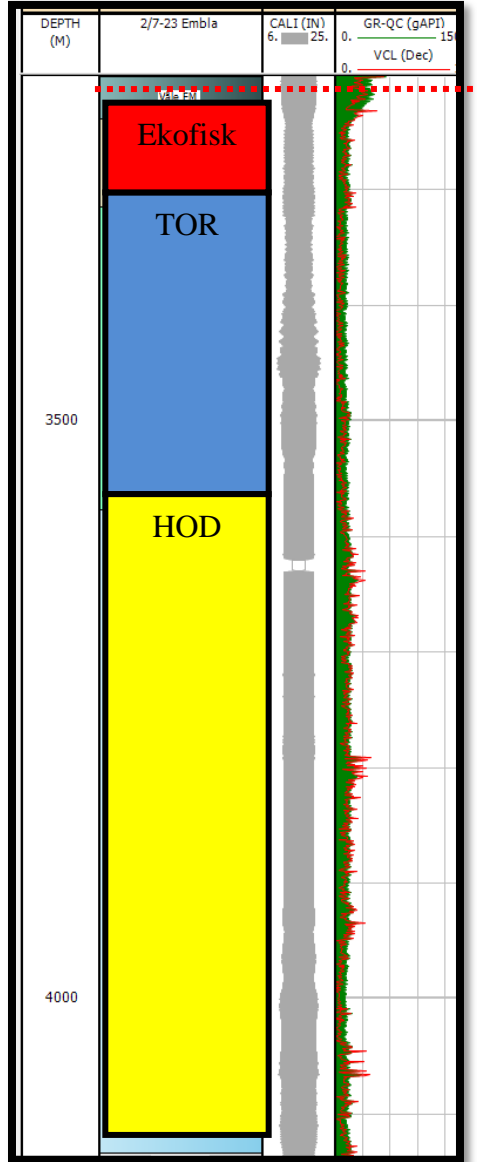


Figure 11: Representation of Tops editing. Red dotted line is top of Ekofisk on npd.no.

Table below is well illustration of list of zone for three wells.

Table 2: List of groups and formation which were encountered in our wells (Norwegian Petroleum Directorate).

<b>Lithologies</b>	<b>2/8-15</b>	<b>2/7-23 S</b>	<b>2/11-9</b>
<b>Nordland Gp</b>	✓	✓	✓
<b>Hordland Gp</b>	✓	✓	✓
<b>Balder Fm</b>	✓	✓	✓
<b>Sele Fm</b>	✓	✓	✓
<b>Balder Fm</b>		✓	
<b>Vale Fm</b>	✓	✓	✓
<b>Ekofisk Fm</b>	✓	✓	✓
<b>Tor Fm</b>	✓	✓	✓
<b>Hod Fm</b>	✓	✓	✓
<b>Blodoks Fm</b>		✓	✓
<b>Hidra Fm</b>		✓	✓
<b>Rodby Fm</b>		✓	✓
<b>Sola Fm</b>		✓	✓
<b>Asgard Fm</b>		✓	
<b>Mandal Fm</b>		✓	
<b>Pre Jassic</b>		✓	
<b>Lista Fm</b>	✓		✓
<b>Tuxen Fm</b>			✓
<b>Carboniferous SST</b>			✓

Table 3: List of well tops of groups and formation in our wells (Norwegian Petroleum Directorate).

	<b>2/8-15</b>	<b>2/7-23 S</b>	<b>2/11-9</b>
<b>Lithologies</b>	Well Tops	Well Tops	Well Tops
<b>Nordland Gp</b>	94 MD	100	115
<b>Hordland Gp</b>	1677 MD	1609	1562
<b>Balder Fm</b>	3044 MD	3090	2937
<b>Sele Fm</b>	3065 MD	3108	2953
<b>Balder Fm</b>		3160	
<b>Vale Fm</b>	3163 MD	3202	3047
<b>Ekofisk Fm</b>	3177 MD	3231	3050
<b>Tor Fm</b>	3346 MD	3315	3091
<b>Hod Fm</b>	3721 MD	3577	3298
<b>Blodoks Fm</b>		4143	3656
<b>Hidra Fm</b>		4150	3661
<b>Rodby Fm</b>		4213	3734
<b>Sola Fm</b>		4301	3795
<b>Asgard Fm</b>		4322	
<b>Mandal Fm</b>		4408	
<b>Pre Jassic</b>		4412	
<b>Lista Fm</b>	3113 MD		2992
<b>Tuxen Fm</b>			3854
<b>Carboniferous SST</b>			4211

#### 4.4 Volume of Clay and Sand Estimation

Clean sand and Clay volume can be estimated by using Gamma Ray because gamma ray measures record of radiation of radioactive material like Uranium, Thorium and Potassium. These radioactive minerals are abundantly present in shale formations. In shale zone gamma ray shows high readings as compare to sand or limestone formations (Rider & Kennedy, 2011). Neutron and Density cross plots colored by Gamma ray log is also another helpful way to find out the V<sub>clay</sub> and V<sub>sand</sub>. Mathematical relations which were used to calculate V<sub>Clay</sub> are given below.

$$V_{Clay} = \{(GR - GR_{Sand}) / (GR_{Shale} - GR_{Sand})\}$$

Or

$$V_{Clay} = \{(NPHI_{env} - \phi \cdot H_f) / (\phi_{Shale})\}$$

## 4.5 Hydrocarbon Corrections

Neutron log provides the record of neutron bombardment with formation which gave measurements in neutron porosity units. In clean and water bearing Limestone neutron porosity equal to true porosity. In other lithologies which will be saturated by hydrocarbon saturated need to be corrected to true values (Rider & Kennedy, 2011). Hydrocarbon correction was applied to sand and limestone which were saturated by hydrocarbons for example Chalks and Pre Jurassic sand of well 2/723S.

### 4.5.1 Methodology

The formulas used to apply corrections in Sand zone having hydrocarbon is given below.

$$NPHIC = (NPHI + 0.04) - V_{cl} * (NPHI_{cl} + 0.04)$$

While in limestone or chalk zone  $NPHIC = NPHI$ .

## 4.6 Effective Porosity Estimation

The porosity of rock which is capable to allow the fluid to flow in rock is known as effective porosity (Gibbs, Barcelona, D, & Lefavivre, 1984). In hydrocarbon bearing reservoirs effective porosity means those pore spaces which are filled by hydrocarbons.



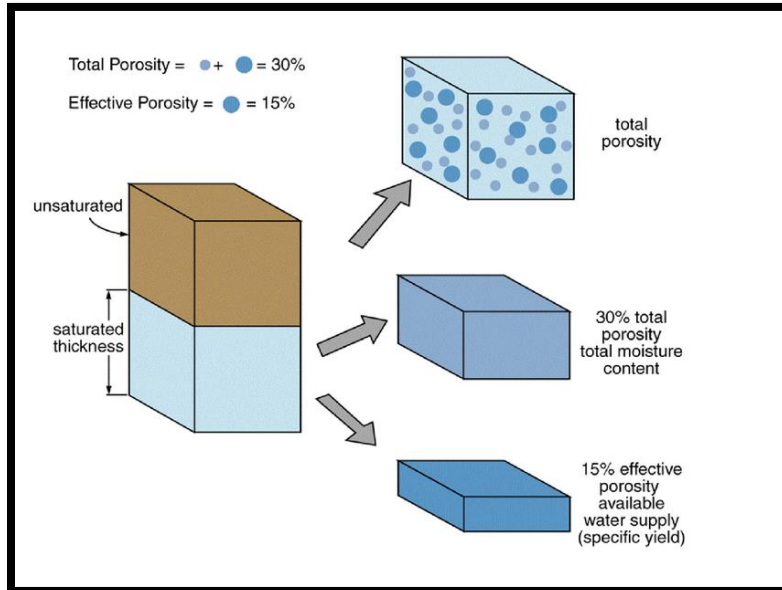


Figure 12: Total and effective porosity (Goolge).

#### 4.6.1 Methodology

Before the estimation of effective porosity, porosity from Density log was calculated by using simple formula given below;

$$PHID = \frac{\rho_{matrix} - \rho_{ob}}{\rho_{matrix} - \rho_{of}}$$

Porosity of clay from density was calculated and the HC correction was applied to estimate the final result of porosity from density log by using following relation;

$$PHID_{cl} = \frac{\rho_{matrix} - \rho_{ob}}{\rho_{clay} - \rho_{of}}$$

$$PHIE = \frac{7 * PHIDC + 2 * NPHIC}{9}$$

### 4.7 Effective Water Saturation

Water saturation is actually the ratio between water column and pore volume while effective water saturation is fraction of water which is correspondence to effective porosity.

#### 4.7.1 Methodology

Water Saturation was estimated by using Archie and Indonesian equations given below. Indonesian equation was used in those zones where volume of clay (VCL) was encountered. While in chalk zones VCL was approximately zero Archie equation was used.

$$S_w = \{(0.62 * R_w) / (\phi^{2.15} * R_t)\}$$

$$S_w = \{(1 / R_t^{0.5}) / (Vcl^{**}(1-(Vcl/2))/Rcl^{**0.5}) + ((\phi^{**} (m/2)) / (a * R_w)^{**0.5})\}$$

#### 4.8 CPI Plots and Conclusion

Final CPI plots were generated after following petro physical frame work. CPI plots (Figure: 13-15) have 10 columns and their names are listed below

1. Depth (m).
2. Zones.
3. Caliper (ft).
4. GR (API) & VCL (Dec).
5. RHOB (gm / cc) & NPHI (DEC).
6. DTSQC (us / ft) & DT (us / ft).
7. SWE (DEC).
8. PHIE.
9. V Clay, V Chalk & V Sand.
10. RT (OHM).

In Figure 13 column number 8 is showing effective porosity, TPHEIT is effective porosity measured after applying Hydrocarbon corrections while PHI is Effective porosity without Hydrocarbon correction in chalk zones.

While in figure 13-15 Column 9 is about Volume of lithologies specially Volume of Chalk, Sand and Clay. A, B and C abbreviations were used for V Sand, V Chalk and V Clay respectively.

After detail analysis of complete logs it was decided to select the Chalk of Ekofisk, Tor, Hod and Hidra formation for the rock physical analysis (Figure: 13-15). In well 2/11-9 gamma ray was showing very high values which was strange and it could be because of borehole mud used during drilling. Ekofisk, Hod and Tor formation were showing 100 percent chalk content while some parts of Ekofisk and Tor formations had some hydrocarbon shows but most of Chalk was

water saturated. The porosity in Ekofisk was good but it was decreasing downward with depth in Hod and Tor formation. While the Hydra formation was showing chalk and little bit clay content (Figure: 13 &15).

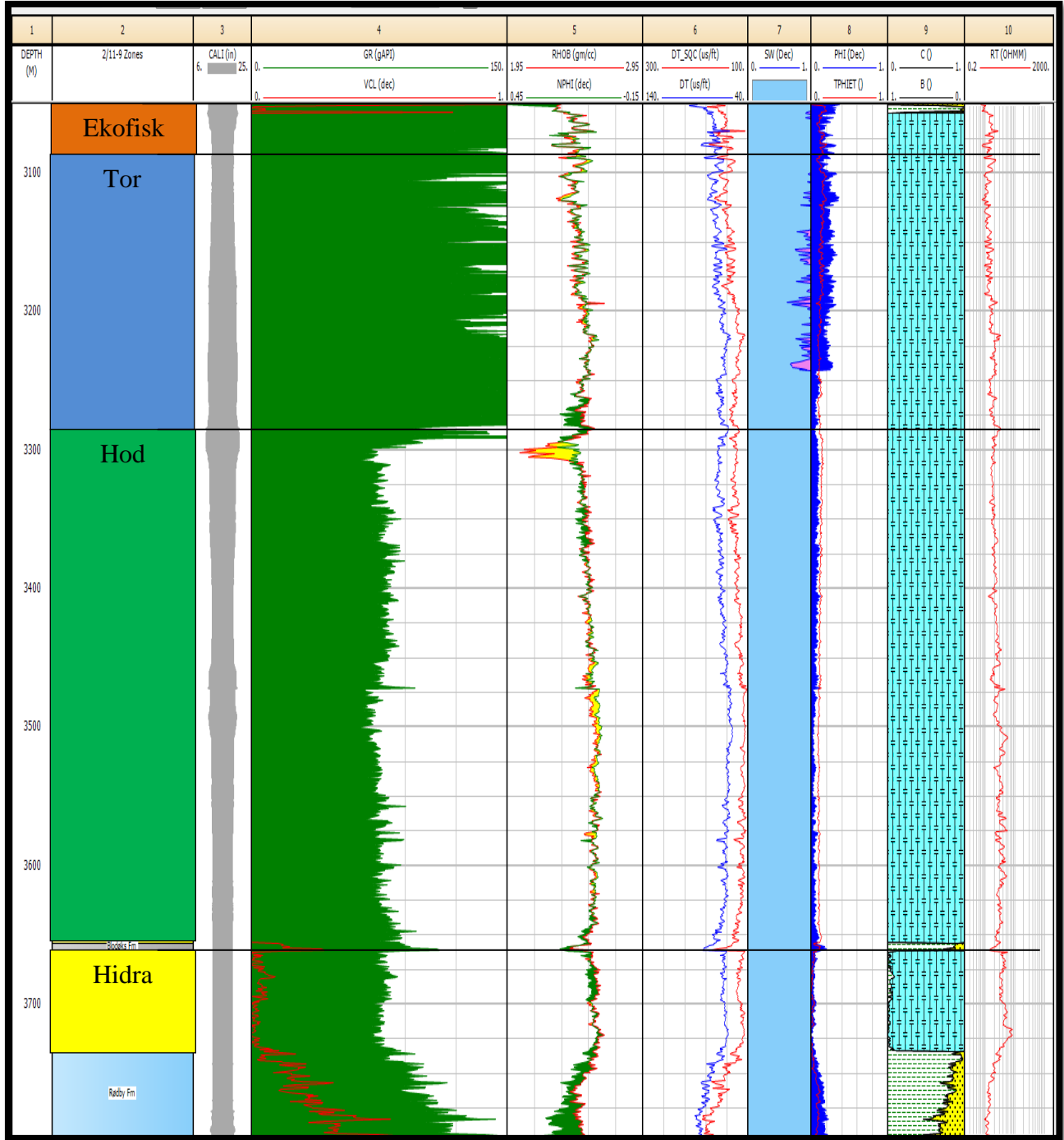


Figure 13: CPI plot of well 2/11-9.

CPI plot of well 2/8-15 is shown in Figure 14, gamma ray in this well was much better and was not much affected by borehole fluids especially in Chalk of Ekofisk, Tor and Hod formations. This well completely saturated by water. The chalk zone of this well had good effective porosity except the Chalk of Hod formation. Resistivity log was showing that well was water saturated.

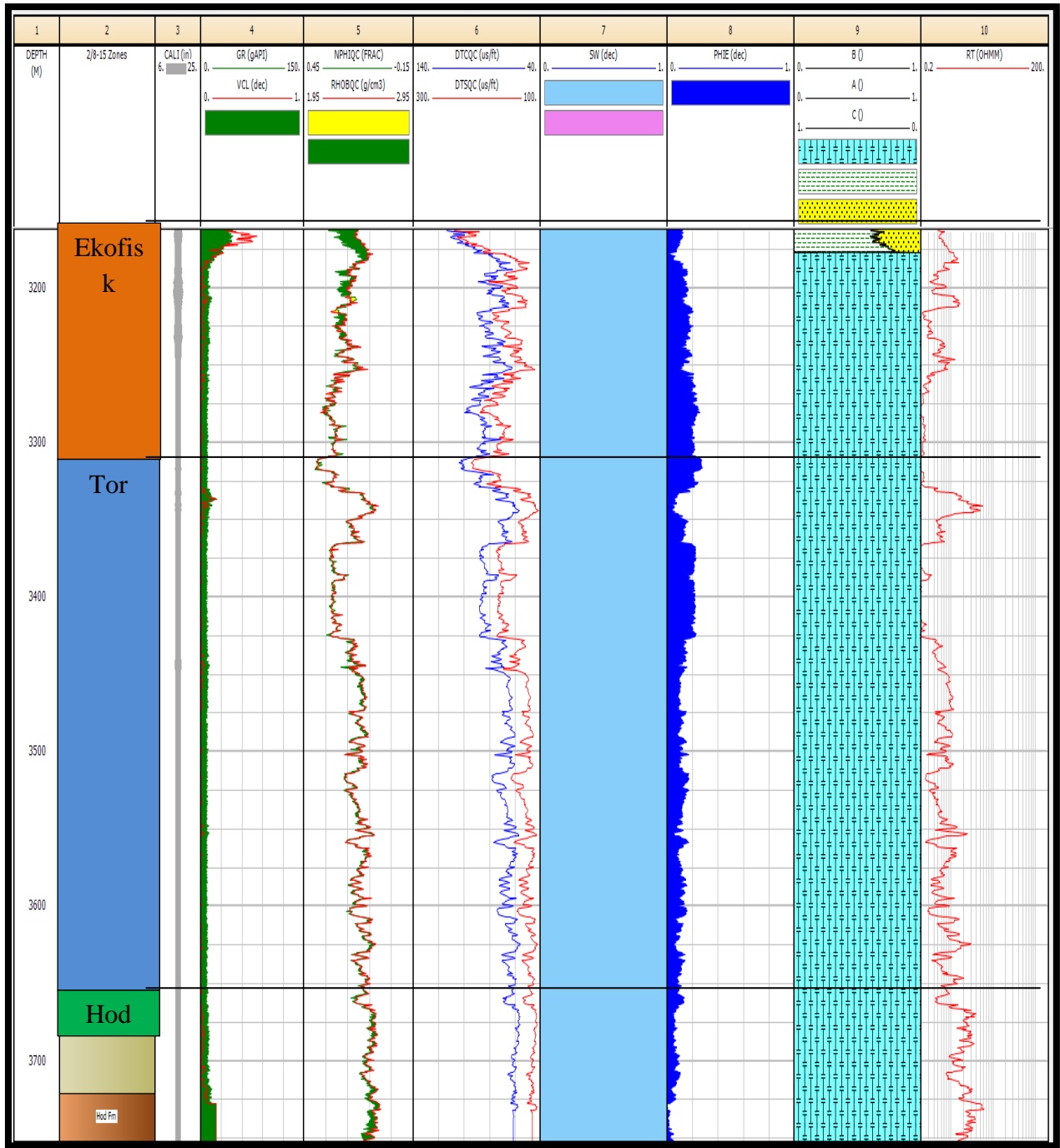


Figure 14: Final CPI plot of well 2/8-15.

Well 2/7-23S was from Embla field. Gamma ray log was much better and was not affected by environment. Sw log shows that it was HC saturated with good reservoir porosity. But Hidra was fully water saturated and the porosity was very low as compare to Ekofisk, Tor and Hod chalk.

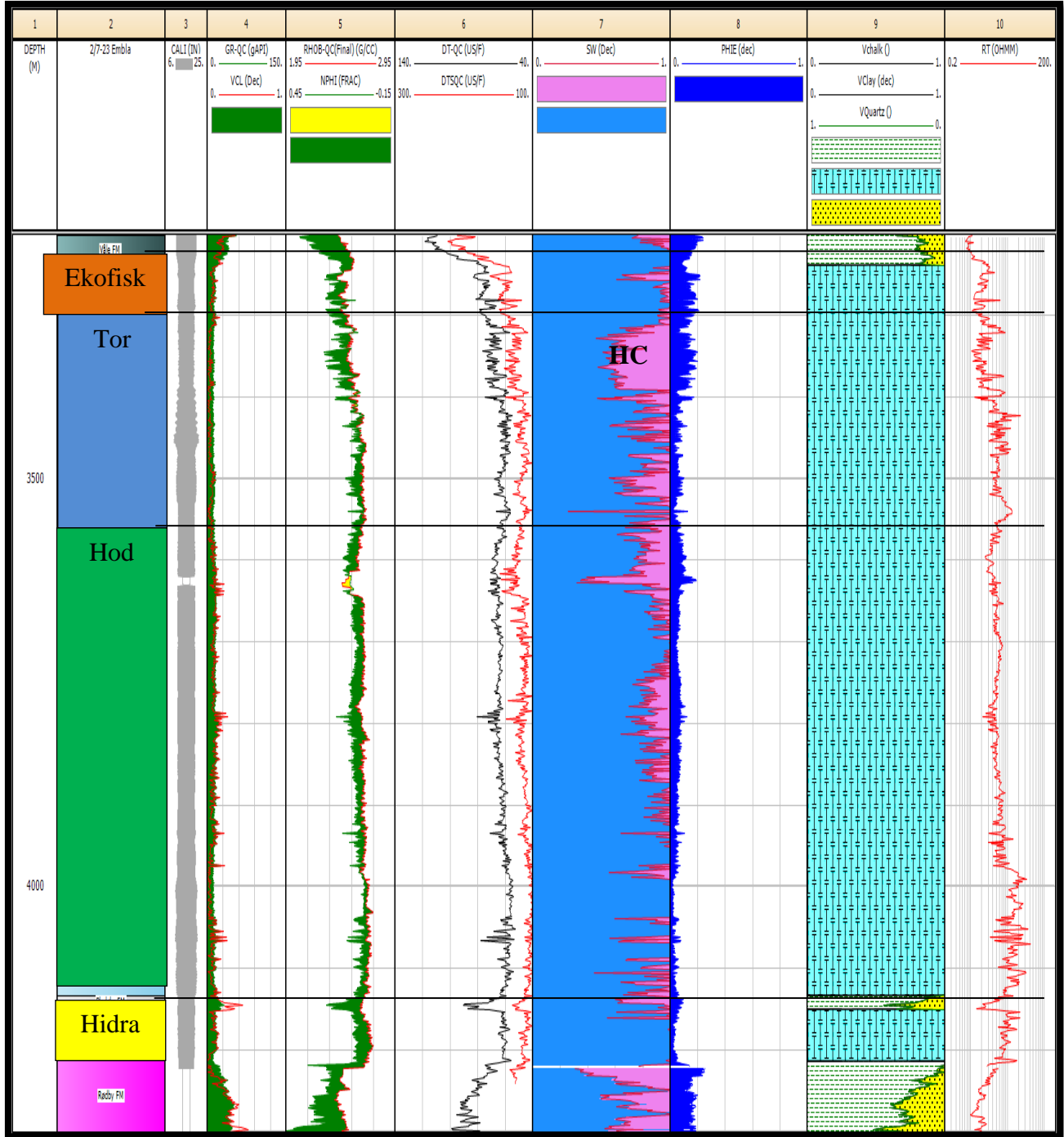


Figure 15: CPI plot of well 2/7-23 S.

Effective porosity of Chalk in well 2/11-9 is from 0.01 to 0.2 ranges (Figure 13), in well 2/8-15 its value is from 0.01 to 0.25 ranges and in Embla (2/7-23S) it ranges from 0.1-0.23 (Figure 15). It was also concluded that water in these wells are very saline which was cause of low resistivity ranges from 0.01-0.001 approximately.

## **5 Rock physics**

### **5.1 Introduction**

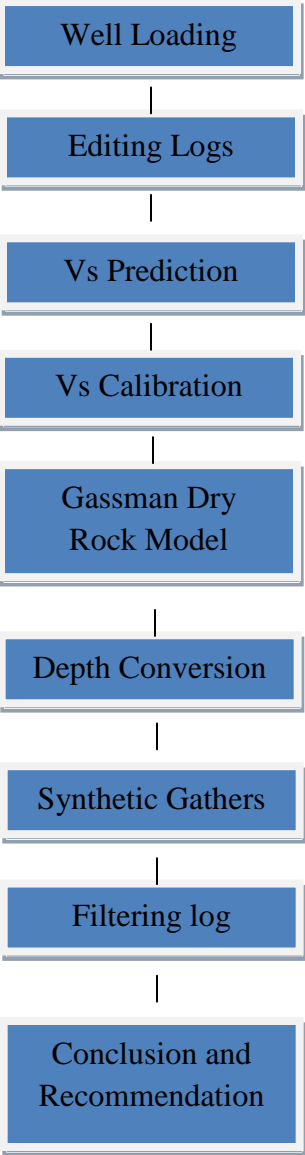
Rocks are generally composed of different minerals and their physical properties depend upon their composition, saturation, pores, cementation and textures etc. Rock physics is the way to relate the geological properties of rocks with their elastic and seismic property (Buland, Seismic Amplitude Analysis And Inversion, 2012). This method helps to predict shear velocities and model the elastic parameters for the new wells or wells with missing shear velocity log.

### **5.2 Rock physical Analysis**

Rock Physics seeks to establish relationship between geological properties of rocks and seismic data response (Dewar, 2001). For Rock physical analysis it is important have good understanding about elastic properties of pore fluid, rock frame and rock fluid interactions etc. (Dewar, 2001). Logs data which were used or usually used to develop best Rock Physical or analysis are sonic (DT) log, shear sonic (DTS) log and density (Rho<sub>b</sub>) log. Other logs like porosities, saturation, V<sub>Clay</sub>, V<sub>Chalk</sub> and other matrix logs are handy logs prepare by Petrophysics to integrate with Rock physical model.

**5.2.1 Methodology and Framework**

Workflow which was adopted for accomplishment of the rock physical analysis is well summarized in flow diagram below.





### **5.2.2 Editing Well logs**

To make better rock physical model it was important to remove the unwanted or noisy data from logs specially  $V_p$ ,  $V_s$  and  $R_{hob}$  logs. There are different ways to check such kind of data but the best approach was used was through generation of cross plots between Depth,  $V_p$ ,  $V_s$  and  $R_{hob}$  etc. This approach was adopted because it is easier to edit problematic zones on cross-plots than on a single log.

### **5.2.3 Depth vs velocities**

Cross plot between depth and Velocities ( $V_p$  and  $V_s$ ) was generated to remove unwanted data especially suddenly high spikes and interpolated values in logs. In the figures 16-19 velocities are on x axis and depth is on y axis. First approach which was adopted to edit only spike and interpolated values but further it was realize that shear velocity values in well 2/7-23 S was missing from Nordland group and some part of Hordland Group. Shear data above Ekofisk zone in well 2/8-15 was not continuous and could lead to miss understanding about the rock elastic properties while well 2/11-9 had complete shear sonic log from top to end of well. Data was color coded with zones to make it simple to identify those zone's colors which were not good.

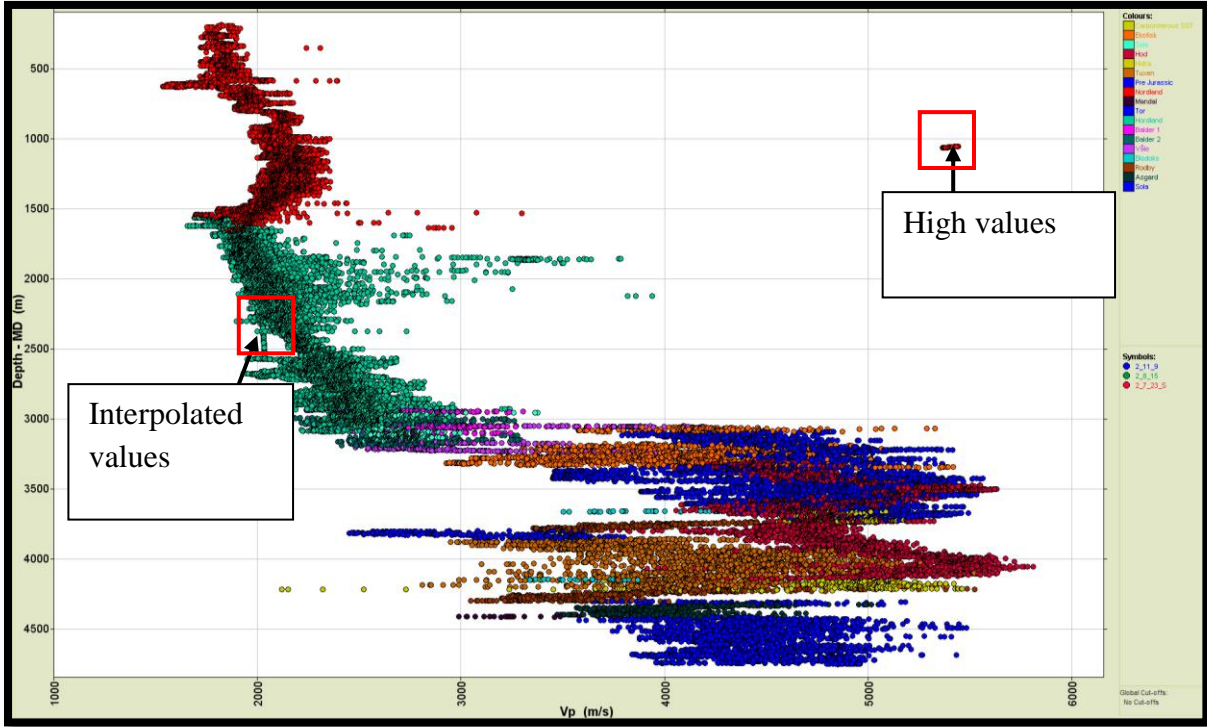


Figure 16: Depth vs primary velocity before editing.

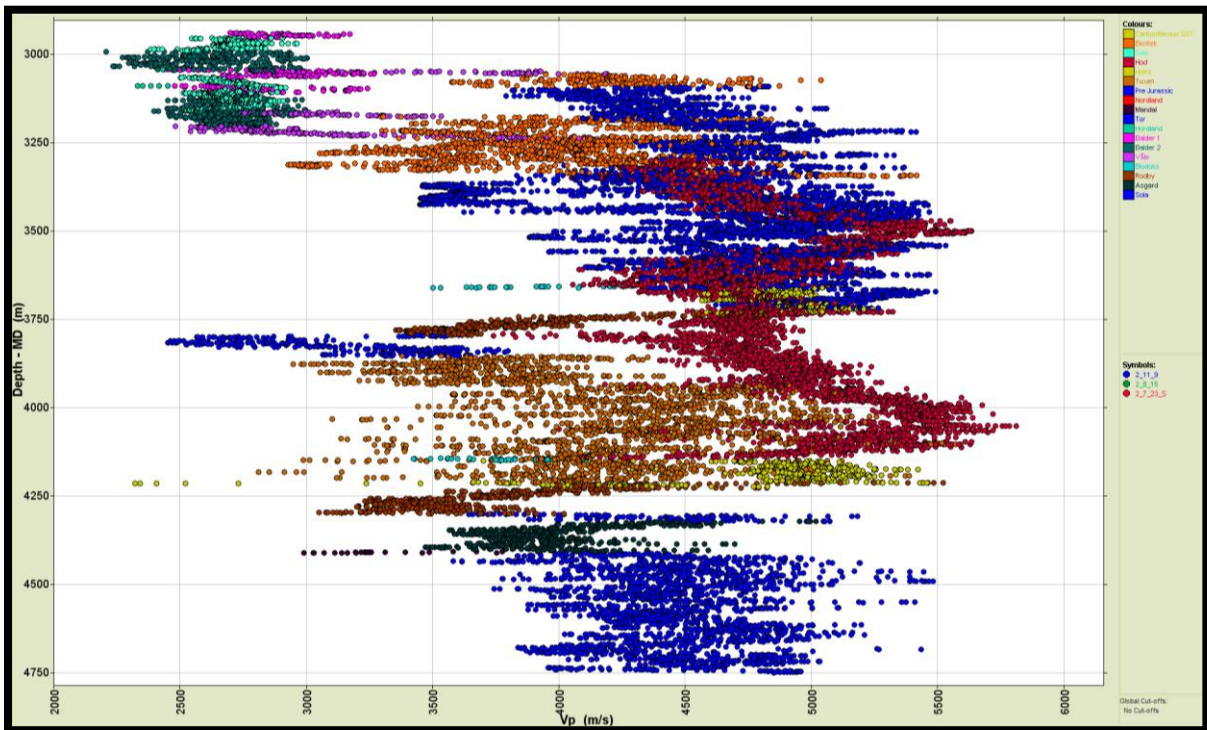


Figure 17: Depth vs P velocity after editing.



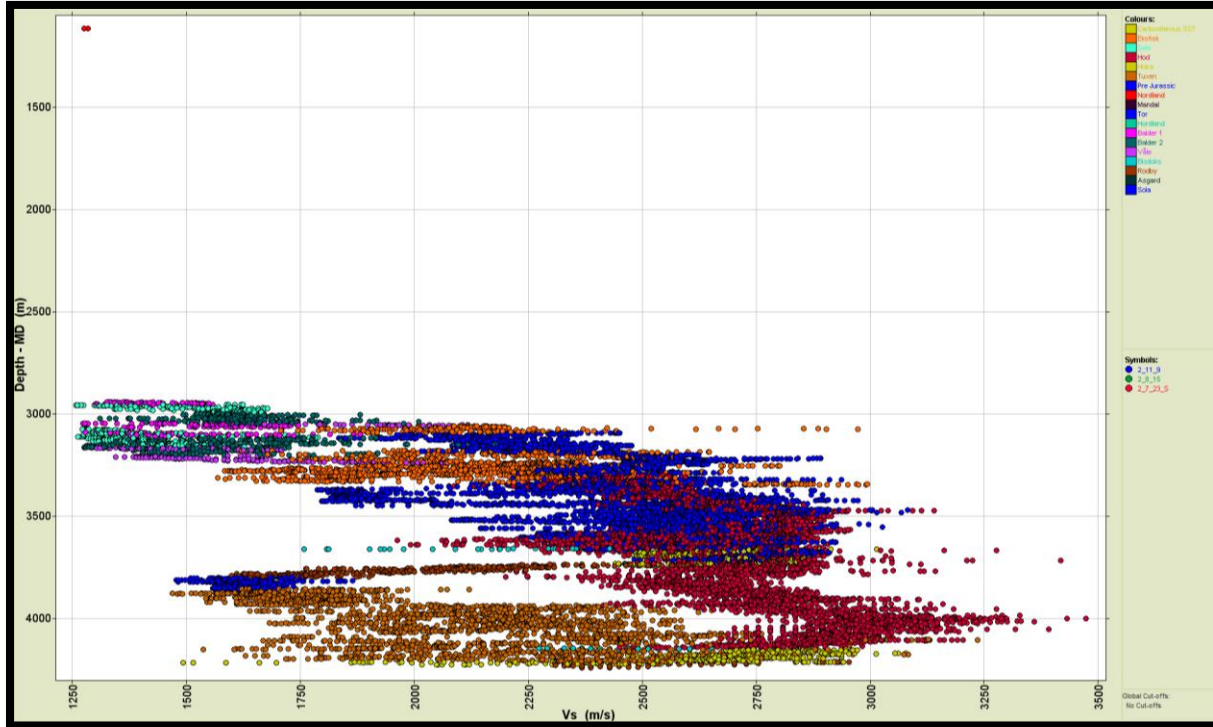


Figure 19: Depth vs shear velocity after correction.

#### 5.2.4 Density vs Velocities

Density versus velocities comparison was done to find out the noisy data from log. The approach was to remove those data which had high density but at that point velocities were low and vice versa. In the figure 20-21 below density is on y axis and velocities are on x axis. The idea was to check those density and velocities points which were not correct and also to see the shear log quality compare to density above Ekofisk and below Hydra zones. Figure 20 is about density and Vs relation before editing unwanted data and polygon is showing those values which are out from AOI. Figure 21 is final representation of shear density relation after editing. Similar idea was adopted for editing primary velocity which was low with respect to density log. Data in figures 20-21 were color coded with color of zones to make it simple to identify those zones which were not good.

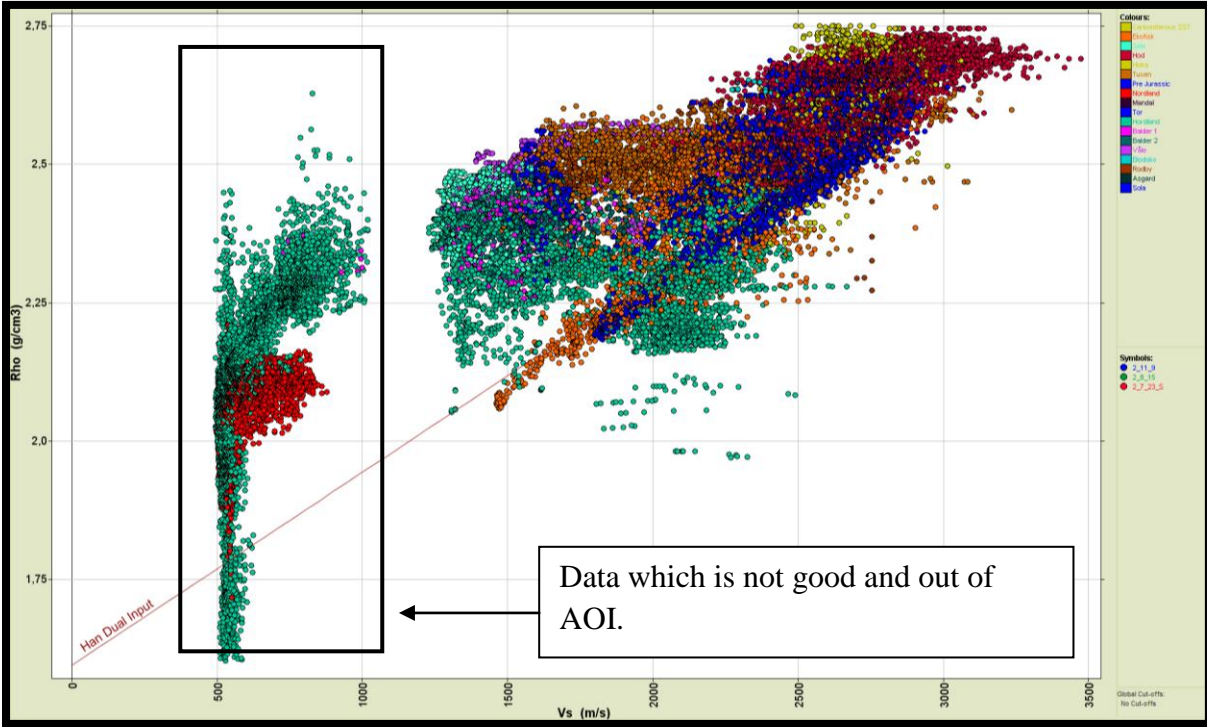


Figure 20: Density versus S- waves velocity before QC.

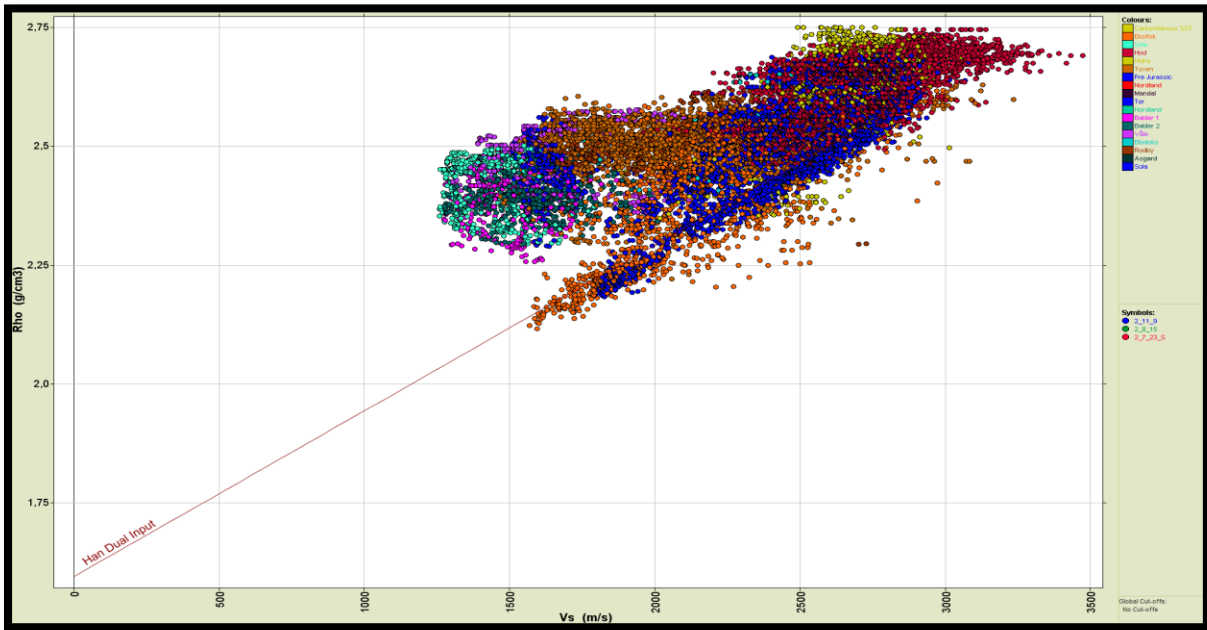


Figure 21: Density versus S- waves velocity before QC.



### 5.2.5 Vp/Vs versus P-Velocity

Cross plot between velocity ratio and primary velocity was generated to edit the values which were below approximately 1.5 Vp/Vs ratio value. In Figure 22 Vp is on x axis while velocity ratio (Vp/Vs) was on y axis. Black dotted polygon in Figure 22 is representing the data which was out of AOI. All the points were color coded with zone's color to easily identify those points which were from our AOI. Red polygons in Figure 22 is representing the unwanted data while figure 23 is final viusaliztion of edited data. Same approach was adopted for shear sonic logs to remove those points which were equivalent points to vp points.

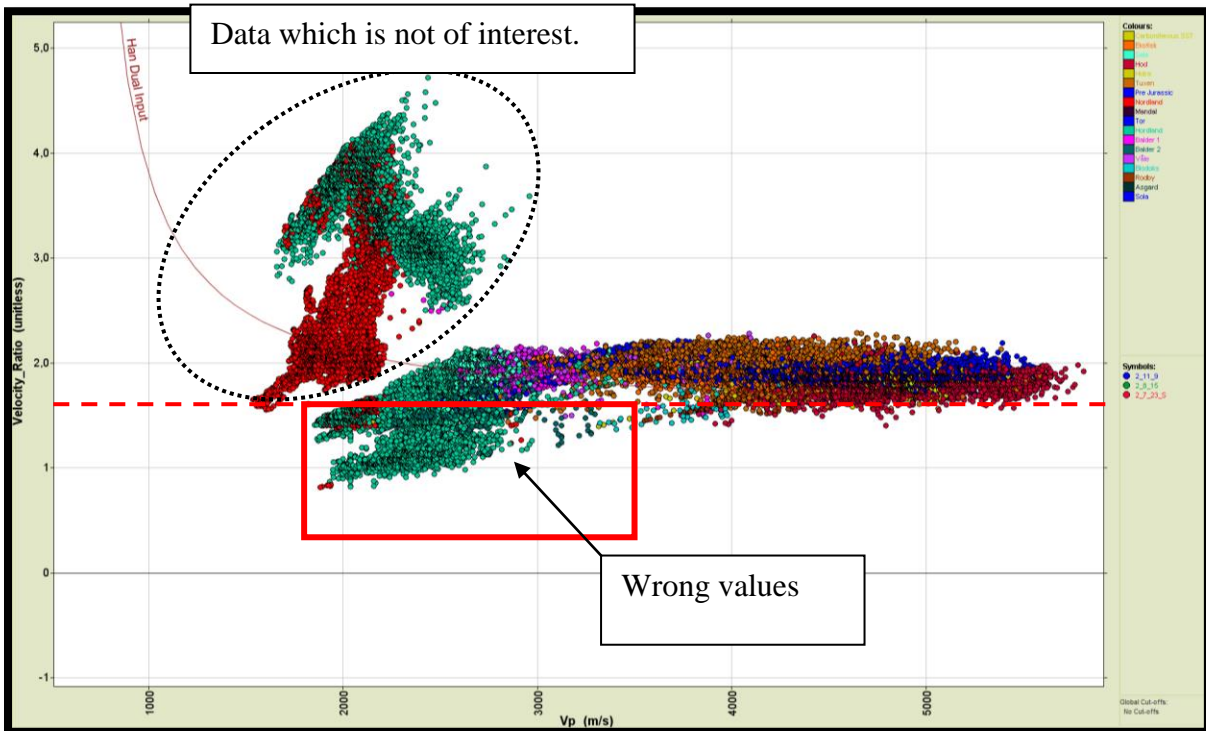


Figure 22: Velocity ratio vs primary velocity before editing.

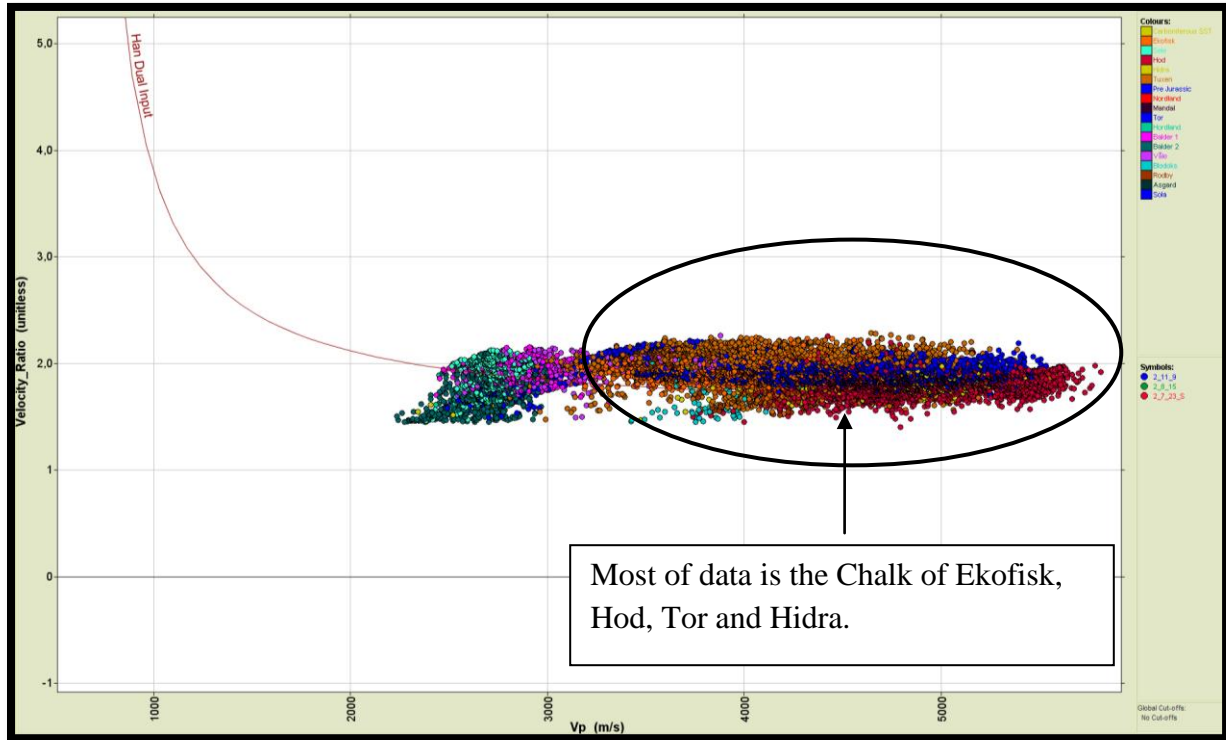


Figure 23: P-velocity versus  $V_p/V_s$  ratio after editing.

### 5.2.6 Velocities Comparison

Shear and primary velocities cross plot was generated to see the best fit trends between these velocities and to find out the wrong velocities values from logs data. Mathematically it is generally believe that shear velocities are approximately half of the primary waves so those shear velocities which were very high at low primary values were removed because velocity their  $V_p/V_s$  ratio was not acceptable according to depth and lithology. In Figure 24  $V_p$  in along x-axis and  $V_s$  are along y-axis while dotted polygons are representing those values which were from area out of interest.  $V_p/V_s$  ratio values usually vary from 1.45 to high range in shallow range but these values are more dependent on lithologies. Points which were showing totally strange values were deleted for example those points which had  $V_p/V_s$  ratio value equal to one.

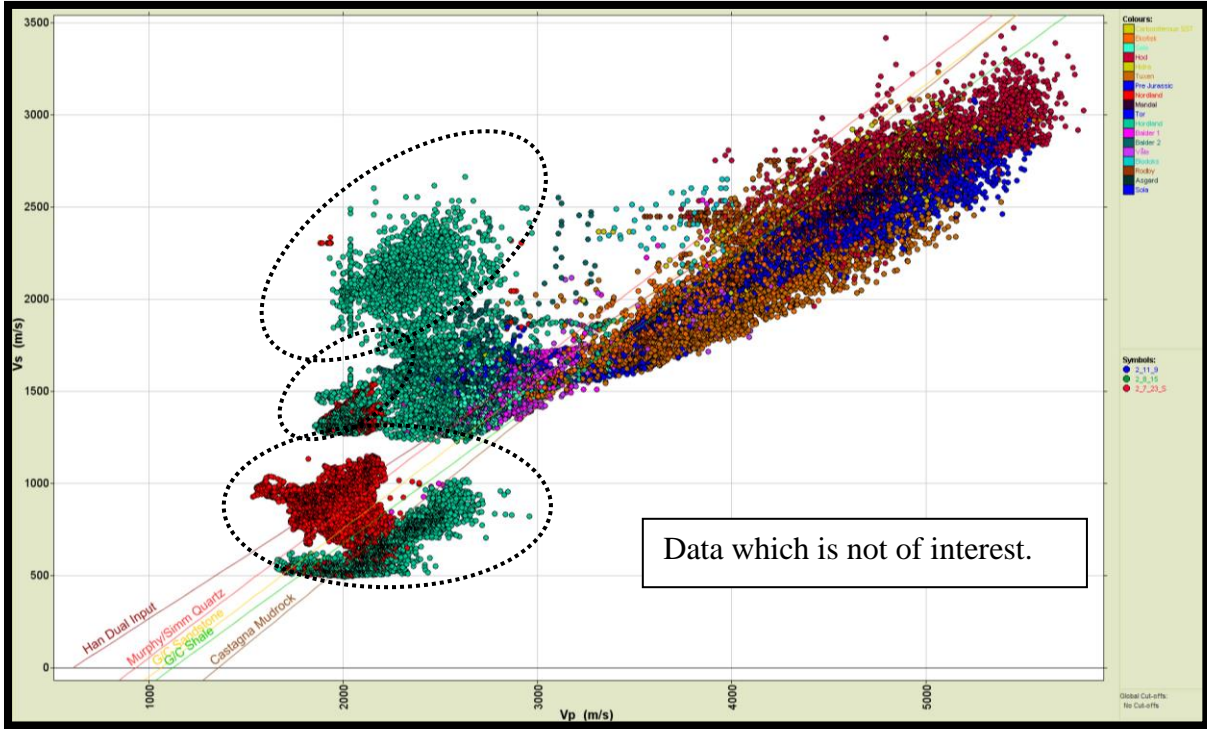


Figure 24: Shear velocity versus primary velocity before QC.

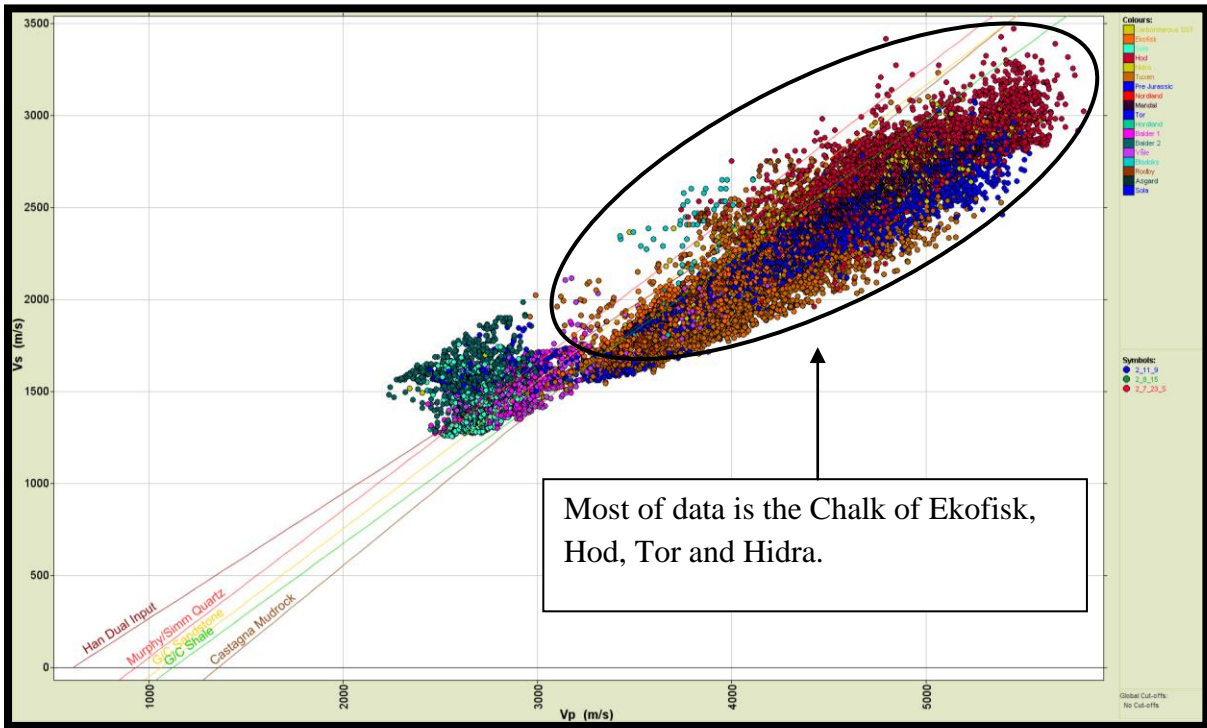


Figure 25: Shear velocity vs Primary wave velocity relation after QC.



### 5.2.7 Vs Prediction

Greensberg Castagna equation (1992) proposed equation to estimate shear velocity (Buland, October 7, 2012) which was used to predict the Vs. Greenberg castagna equation actually depend on lithologies and effect the coefficients used in equations. Equations in case of different lithologies are listed below.

$$V_s = aV_p + b \text{ (Clastic rocks)}$$

$$V_s = -a_{i2} V_p^2 + a_{i1} V_p - a_{i0} \text{ (Limestone rocks)}$$

In these equations a, b,  $a_{i2}$ ,  $a_{i1}$ ,  $a_{i0}$  are the constants and their values can vary (Buland, Seismic Amplitude Analysis and Inversion, 2012)but standard values of these constant for different lithologies are listed in table 4. It depends on the results of modeled Vs. Vs and Vp plot was used to get the coefficients value for sandstone, shale and limestone lithologies. Greenberg Castagna was used to predict shear velocity (Figure 26) red log is modeled shear velocity log.

**Table 4: List of regression coefficients in pure lithologies according to Greensberg Castagna 1992 (Buland, October 7, 2012).**

<b>Lithologies</b>	<b><math>a_{i2}</math></b>	<b><math>a_{i1}</math></b>	<b><math>a_{i0}</math></b>
<b>Shale</b>	0	0.76969	-0.86735
<b>Sandstone</b>	0	0.80416	-0.85588
<b>Limestone</b>	-0.05508	1.01677	-1.03049
<b>Dolomite</b>	0	0.58321	-0.07775

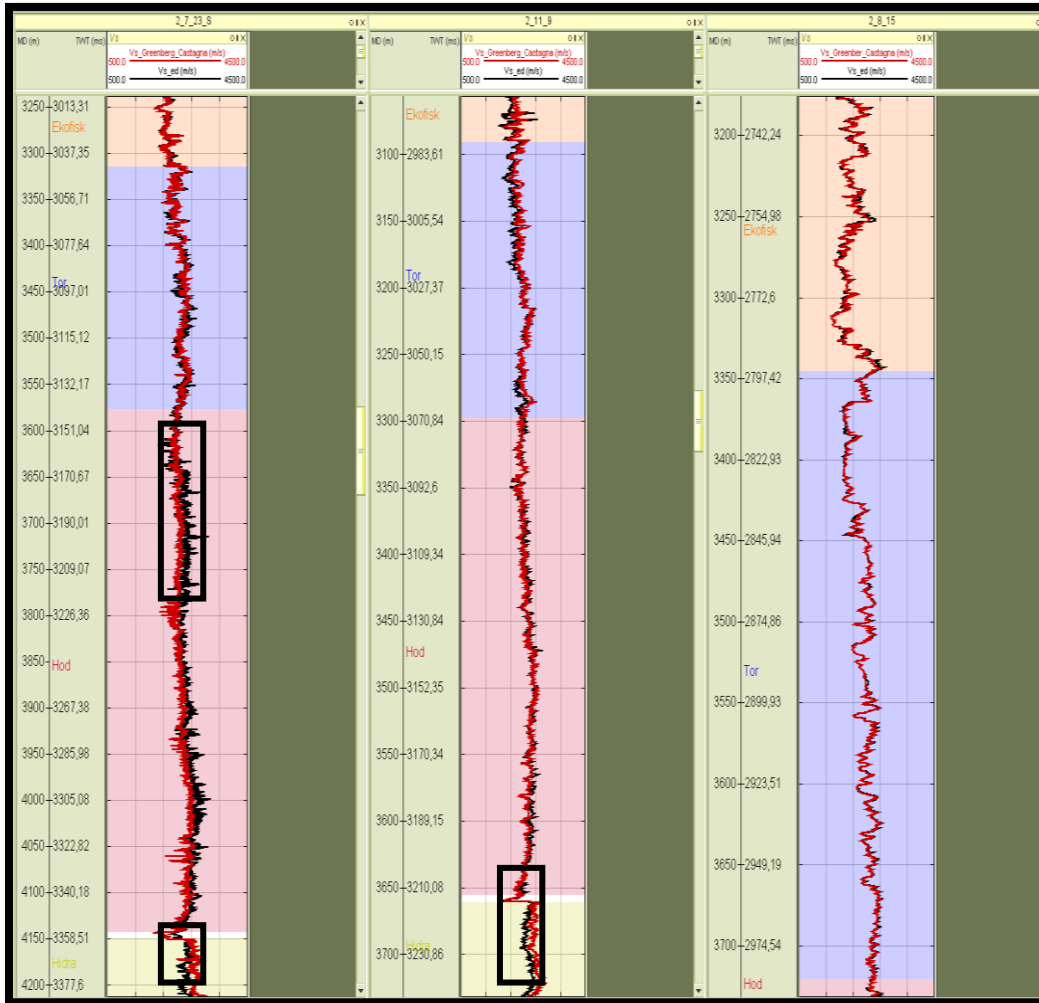


Figure 26: Model shear waves through Greensberg Castagna equation (in red).

### 5.2.8 Vs Calibration

It was found that modeled Vs at some areas was different as compare to measured shear velocity log (Figure 26) especially in Hydra formation of well 2/723 S and 2/11-9. Predicted shear velocity was calibrated by making different cross plots to see trends for different lithologies. The trends in intervals where Vs was not estimated properly was fixed by making better trend line and calculating the new coefficient to find good results. In Figure 27 it can be clearly seen the difference between simple model and calibrated model shear velocity log. Figure 28 is showing the well correlation between measured and model shear velocity after calibrating the model shear velocity.

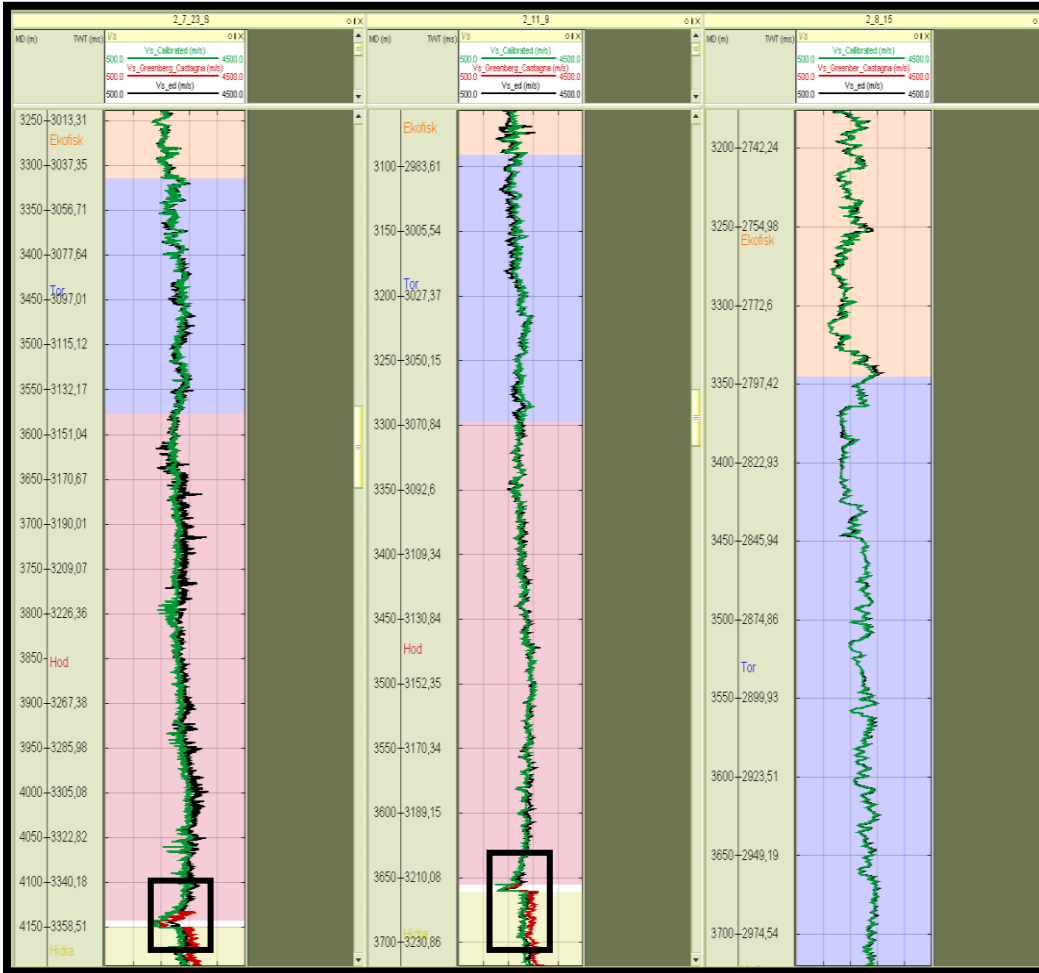


Figure 27: Model Vs after calibration (in green).

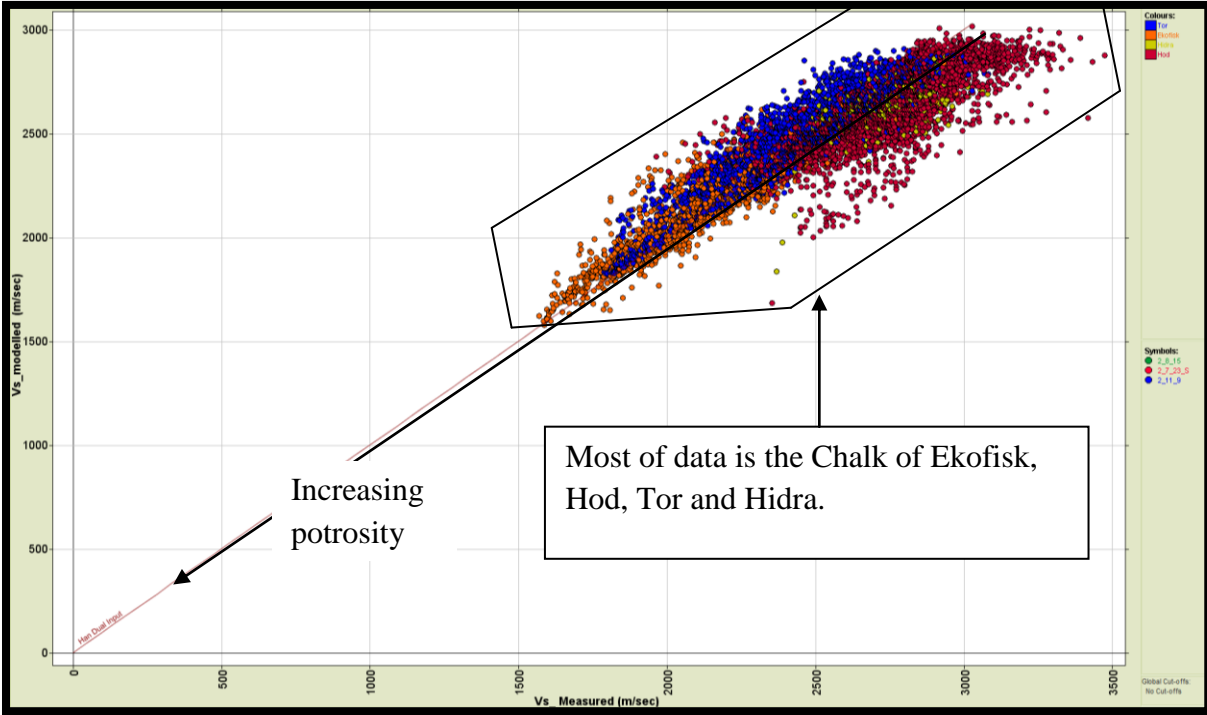


Figure 28: Correlation between model and measured  $V_s$ .

### 5.2.9 Gassman Fluid Substitution

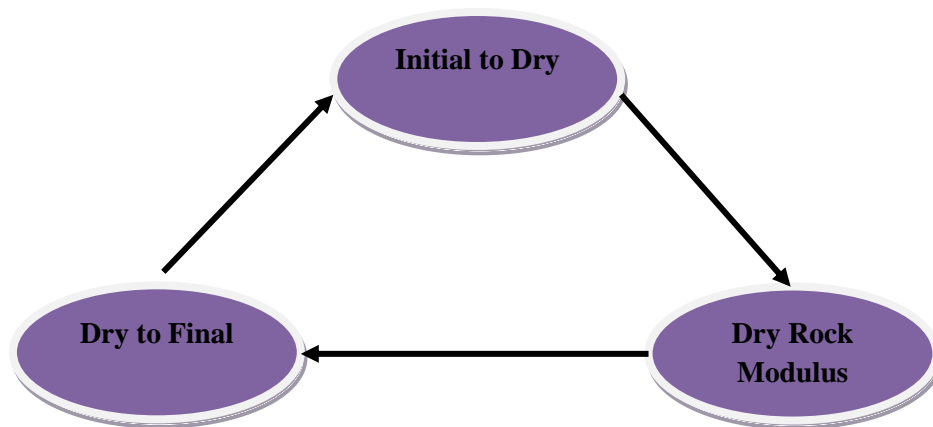
Hydrocarbons exploration is the important target in the Seismic Exploration Industry. Therefore to reach the target more precisely it is important to understand the behavior of rocks when they are porous and saturated with the fluids like oil, gas and water. Mostly Gassman equation is used for rock physical modeling of sandstone but for shale and carbonate it is risky to use because of their deviation from theory (Buland, October 7, 2012). As in our case risk was taken for chalk reservoirs to get well understanding. Change in bulk density and compressibility of rocks are fluids effecting factors which need to be consider carefully (Per Avseth, Tapan Mukerji, & Gary Mavko, 2005). Gassman equation is used to calculate effect of fluids on elastic properties of fluid saturated rocks. Fluid could be brine, oil and gas but pores can be empty (Buland, Seismic Amplitude Analysis And Seismic Inversion, 2012). In Gassman equation application it is assumed that rock is homogeneous, isotropic and pores are connected (Buland, Seismic amplitude analysis and Seismic Inversion, 2012).

### 5.2.9.1 Estimation of Parameters

For the calculation of Gassman fluid substitution in water, oil and gas cases it was important to calculate the primary velocity, secondary velocity and  $\rho_{ob}$  of different lithologies specially Shale, Sand and Chalk. These parameters were calculated by making cross plots of Velocities and densities with porosity.

#### 5.2.9.1.1 Methodology & Framework

Main steps or frame work which was adopted is available in workflow below.



Important parameters which were required for the accomplishment of Gassman equation are listed below

- Logs
- Initial Fluid
- Working Intervals
- Cut-off

First it was important to define the body for which fluid substitution was going to be performed. Selection of porosity and saturation log was important to decide before proceeding. Effective porosity and water saturated logs were used because of unavailability of total porosity and

saturated logs. For defining the body refined values of Vp, Vs, Rhob, effective porosity, initial fluid saturation logs were used. To make proper mineral set for the body it was important to calculate Vp, Vs, Rho, Ko, Mu and M. Which was done by making cross plot of Vp, Vs and Rhob versus porosity to find their values in case of PHIE equal to zero (Figure 29 ). Red highlighted polygon is shown in figure 26 to represent new calculated parameters for body.

Type	Ko	Mu	Rho	M	Vp	Vs
Quartz	21,923	13,042	2,68	39,313	3 830	2 206
Shale	23,314	12,143	2,73	39,504	3 804	2 109
Calcite	53,306	26,57	2,7	88,733	5 732,71	3 437
Dolomite	94,9	45	2,87	154,9	7 346,572	3 959,728
Chert	26	32	2,35	68,667	5 405,54	3 690,125
Aragonite	47	39	2,94	99	5 802,885	3 642,157
Magnesite	114	68	3,01	204,667	8 245,943	4 753,037
Na-Feldspar	55	28	2,62	92,333	5 936,475	3 269,101
K-Feldspar	48	24	2,56	80	5 590,17	3 061,862
Ca-Feldspar	85	38	2,73	135,667	7 049,45	3 730,873
Muscovite	52	31,5	2,82	94	5 773,503	3 342,187
Biotite	50	27,5	3	86,667	5 374,838	3 027,65
Halite	25,2	15,3	2,16	45,6	4 594,683	2 661,453
Anhydrite	66,5	34	3	111,833	6 105,553	3 366,502
Gypsum	58	30	2,31	98	6 513,389	3 603,75
Pyrite	158	149	5,02	356,667	8 429,065	5 448,052
Dry Clay	27	17	2,68	49,667	4 304,92	2 518,588
Other 1	0	0	0	0	0	0
Other 2	0	0	0	0	0	0
Other 3	0	0	0	0	0	0
Siderite	123,7	51	3,96	191,7	6 957,664	3 588,703
Glauconite	15	10	2,67	28,333	3 257,566	1 935,282
Orthoclase	17,96	32,41	2,52	61,173	4 926,98	3 586,239
Plagioclase	55,8	33,3	2,59	100,2	6 219,908	3 585,686
Hornblende	87	43	3,12	144,333	6 801,521	3 712,419

Figure 29: Estimated values of Vp, Vs and Rho.

Dry rock plot (Figure 30) helps to correct the results of initial dry rock calculation. The purpose was to estimate best parameters to bring maximum data inside upper and lower bounds of dry rock model shown in figure 30 below. Stiffness lines were used to check the quality of data. Data which was acceptable is highlighted in blue color while those points which were not acceptable are shown in grey color and they are outside the bound. Upper and lower bounds are shown in figure 30 while points highlighted by red polygon are representing the effect of HC.

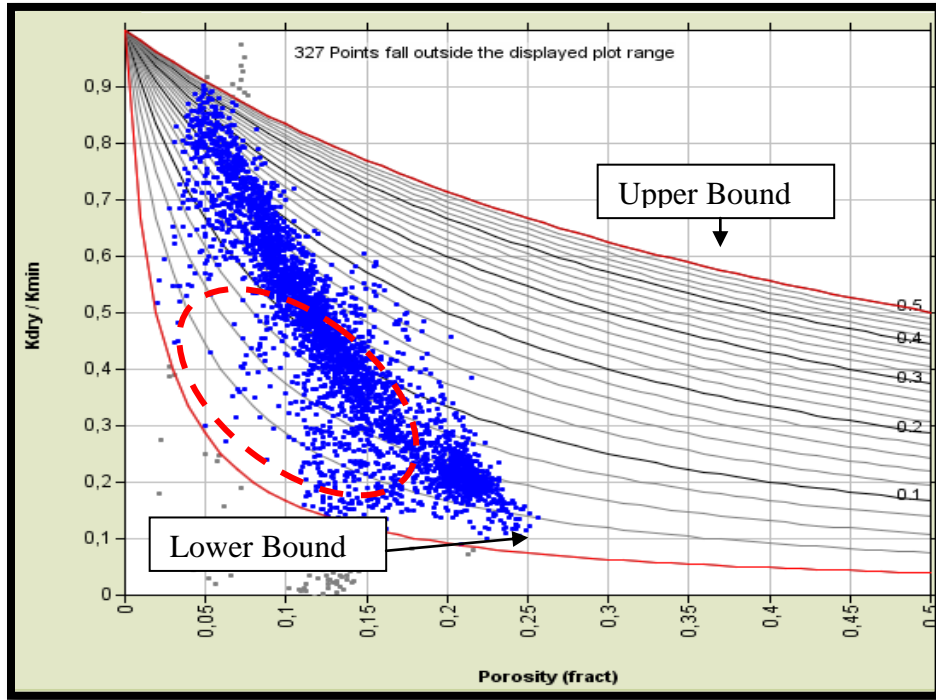


Figure 30: Dry rock plot of Chalk inside the upper and lower bound after calibration.

### 5.2.10 Scenarios & Seismic Gathers

Three different scenarios (Figure: 31) of shear velocity were generated to see effect of porosity in case of saturation with different fluids. There was good correlation between measured and modeled Vs in all cases.

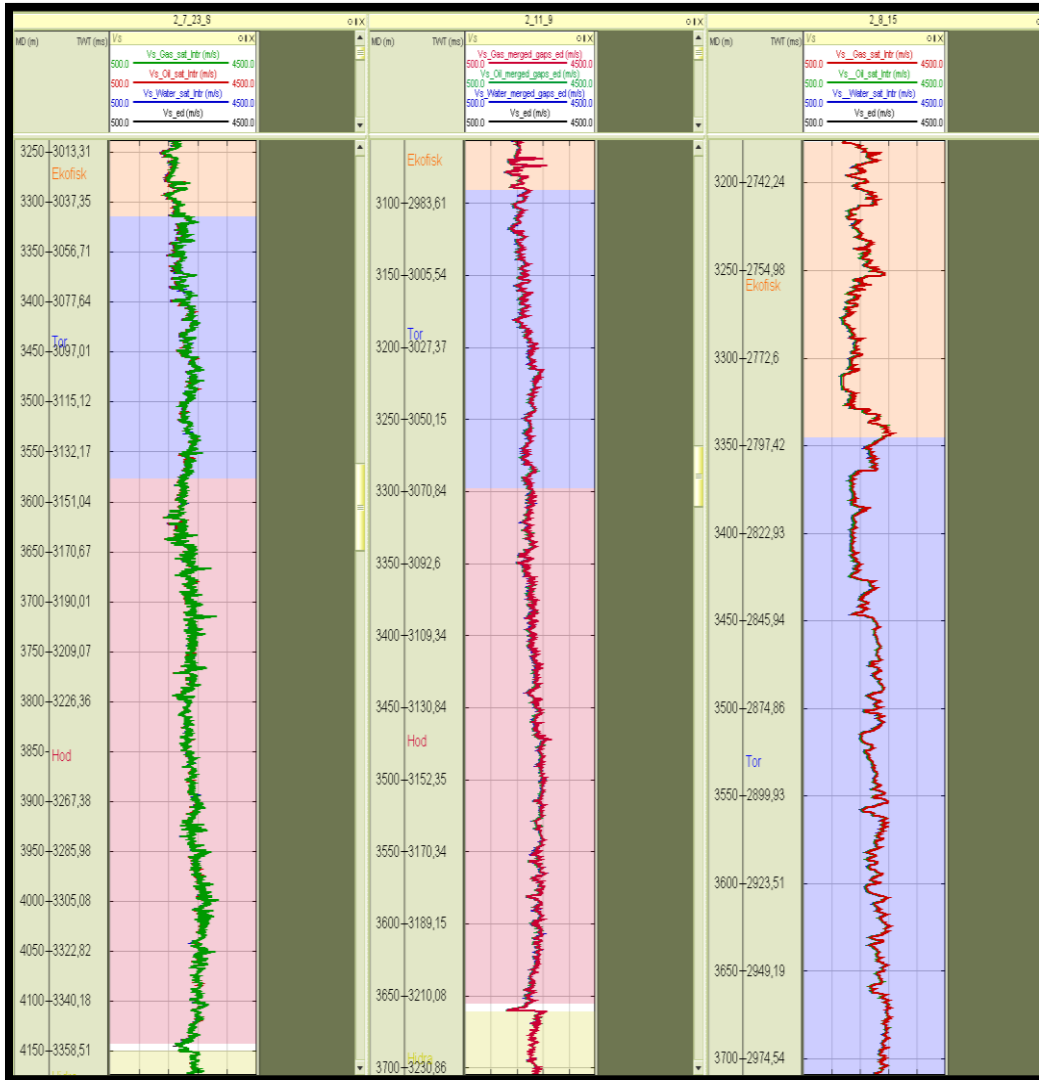


Figure 31: Three scenarios of model Vs logs in case of oil (green), gas (red) and water (blue) saturation comparison with well 2/7-23S, 2/11-9 and 2/8-15 from left to right.



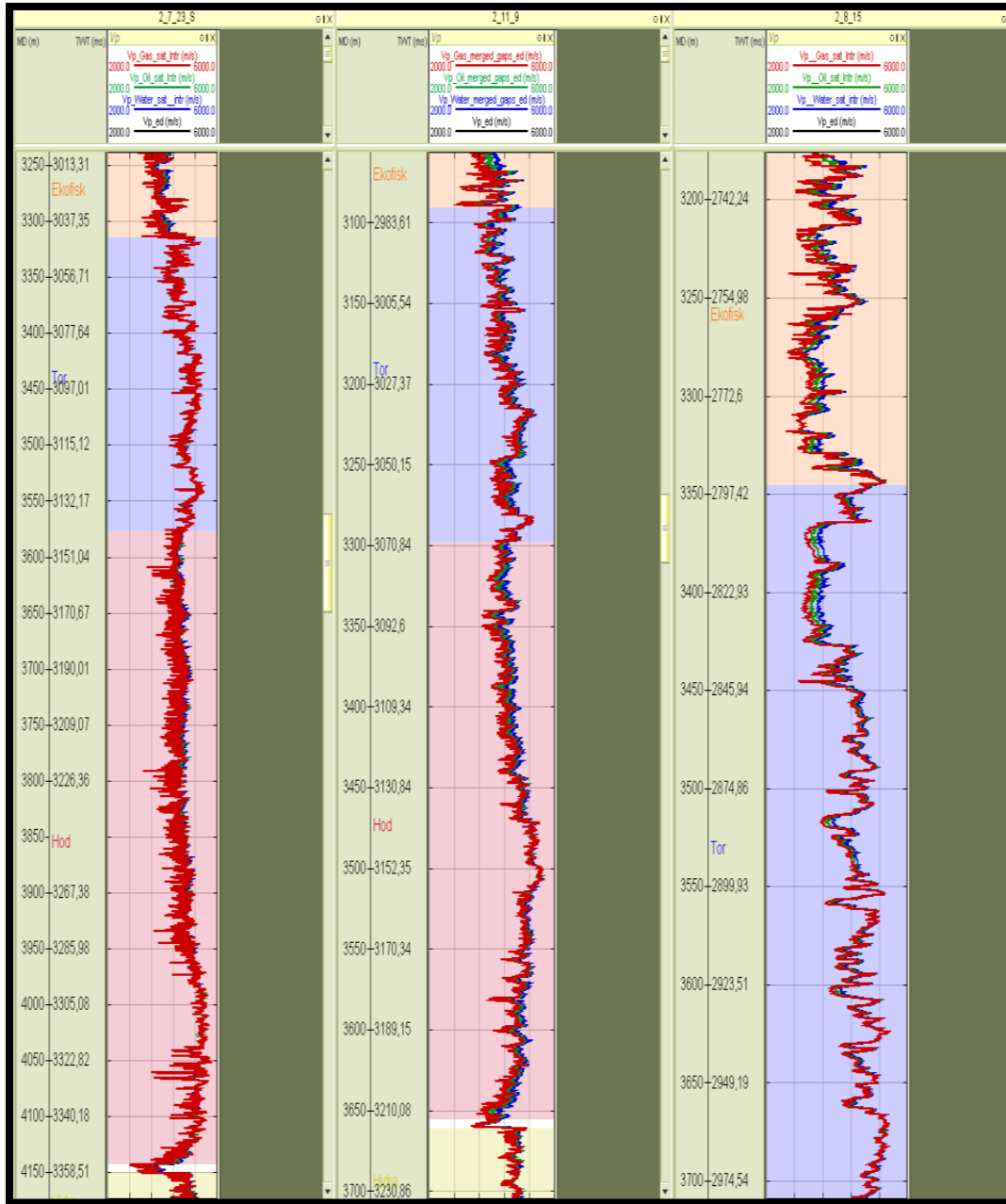


Figure 32: Three scenarios of model Vp logs in case of oil (green), gas (red) and water (blue) saturation comparison with well 2/7-23S, 2/11-9 and 2/8-15 from left to right.

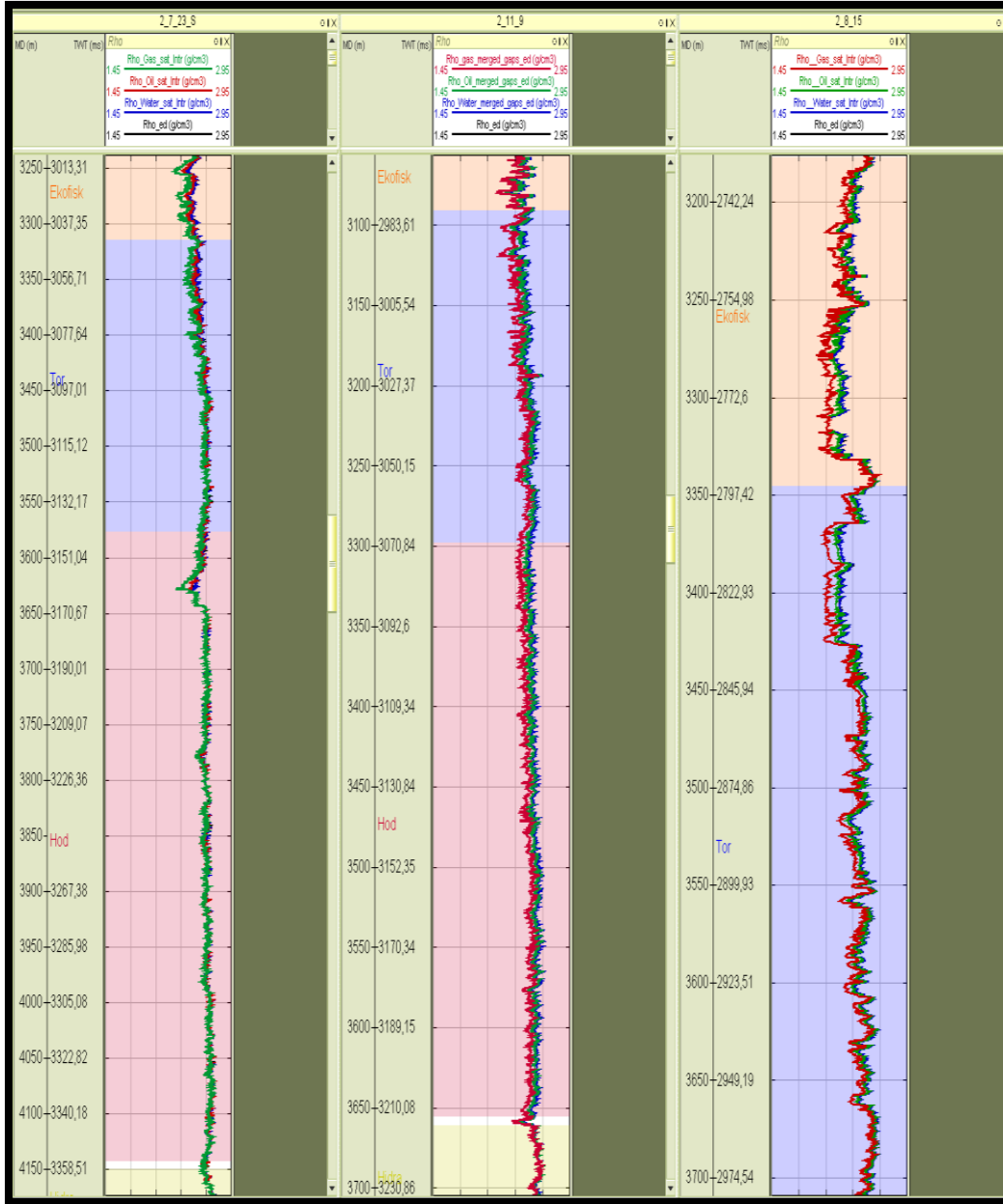


Figure 33: Density log scenarios in case of oil (green), gas (red) and water (blue) saturation comparison with well 2/7-23S, 2/11-9 and 2/8-15 from left to right.

These measured logs were filter according to seismic resolution to get understanding about measured and modeled shear velocities in same domain which is showing very good correlation between each other. In figures below (34-36) it was observed that shear velocity log was not showing variation with change of fluid type in Chalk formations while primary velocity logs (Vp) was showing variation at some part and at some areas there were no variations. That is dividing

the chinks in two different kind according to their trends observe in logs. This could be because of low or high porosity and low or high liquid saturation respectively. For example in figure 34  $V_s$  is increasing where porosity is low and decreasing where porosity is high but primary velocity is not much disturb. But overall in chalk modeled  $V_s$  showing wavy variations and it is difficult to say something confidently about such behavior. It could be cause of porosity and fluid effect because chalk has secondary porosity and in these areas chalk has fractured porosity.

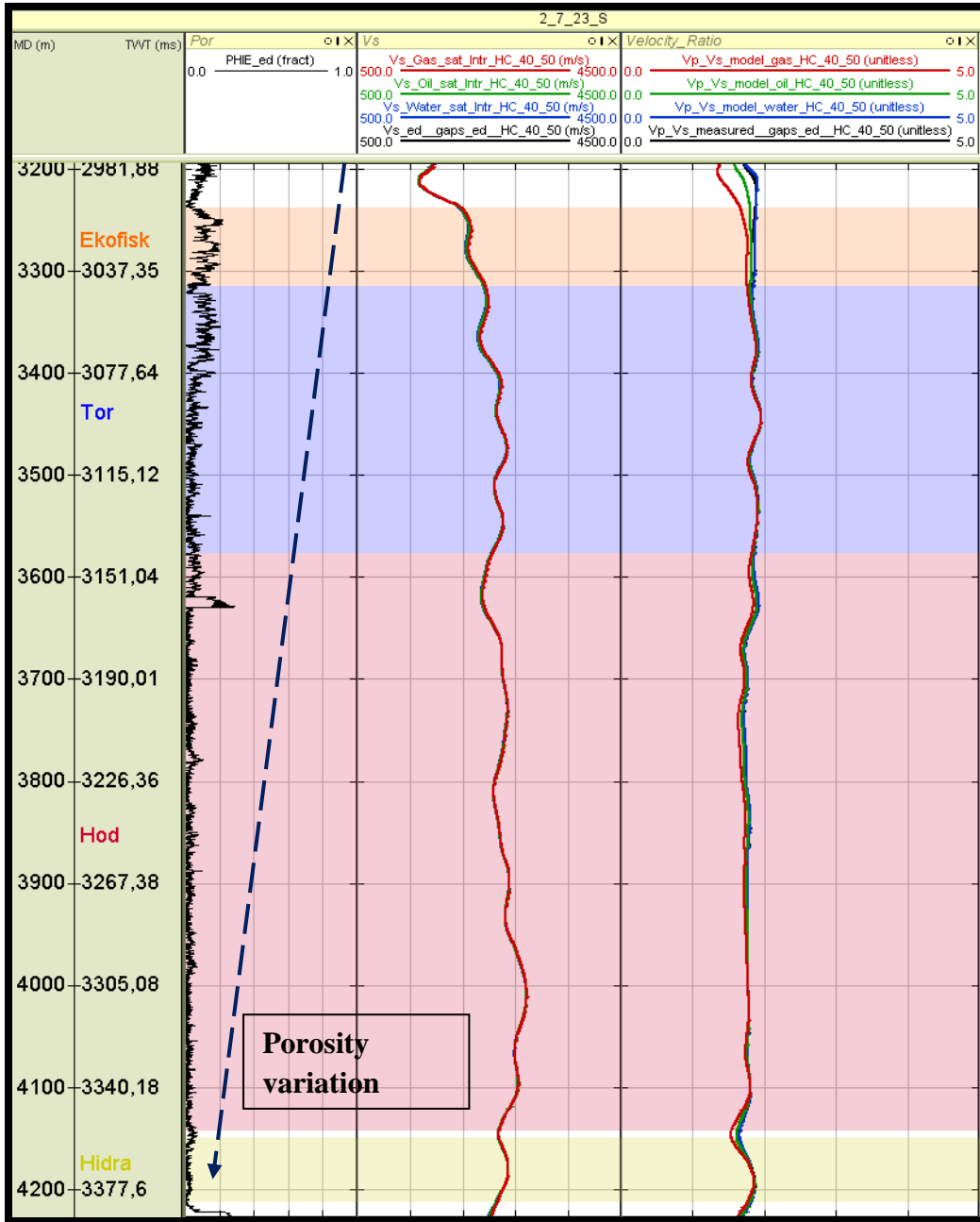


Figure 34: Three different fluids saturated filter logs (Well 2/7-23 S), oil (green), gas (red) and water (blue) saturation.

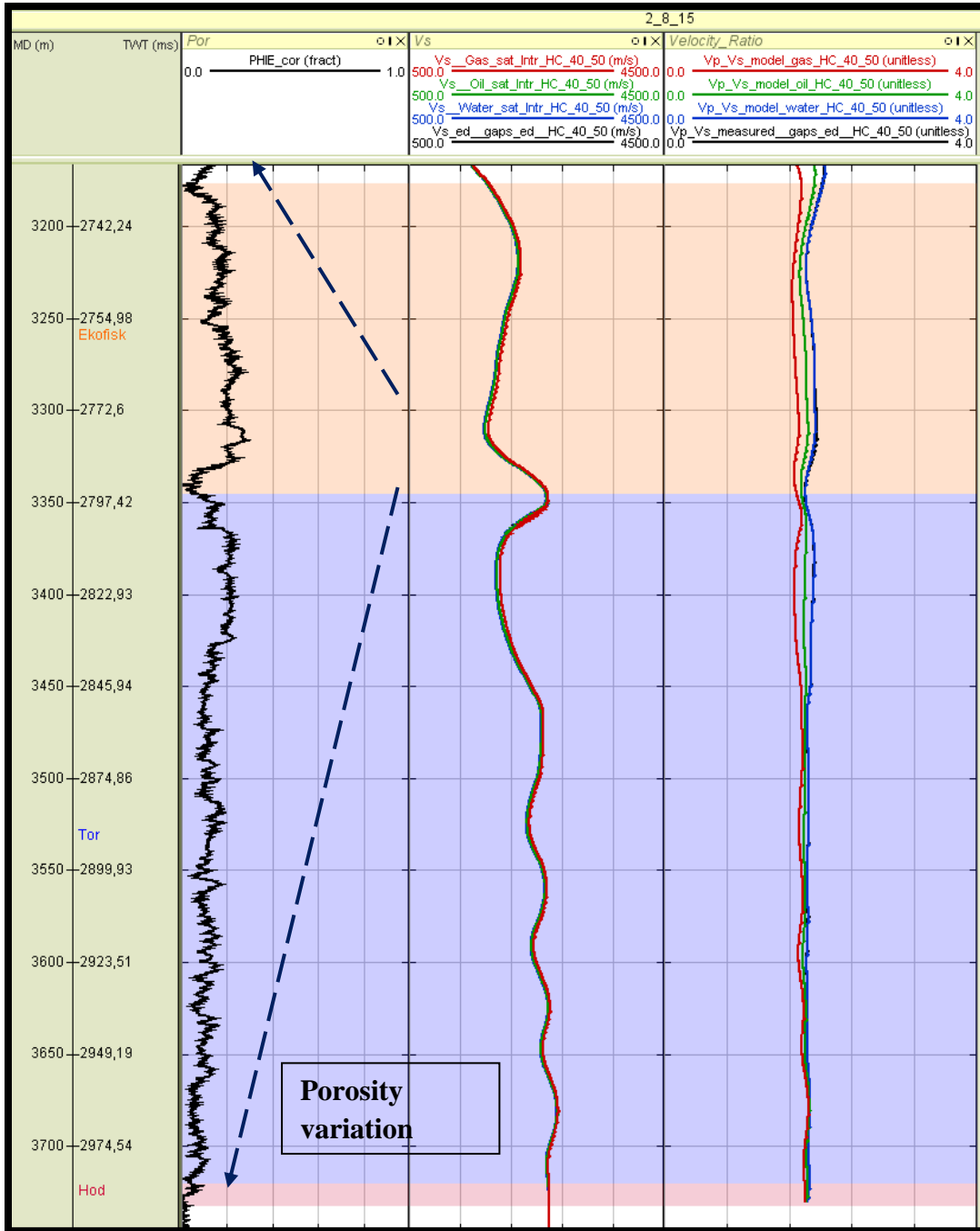


Figure 35: Three different fluids saturated filter logs (Well 2/8-15), oil (green), gas (red) and water (blue) saturation.

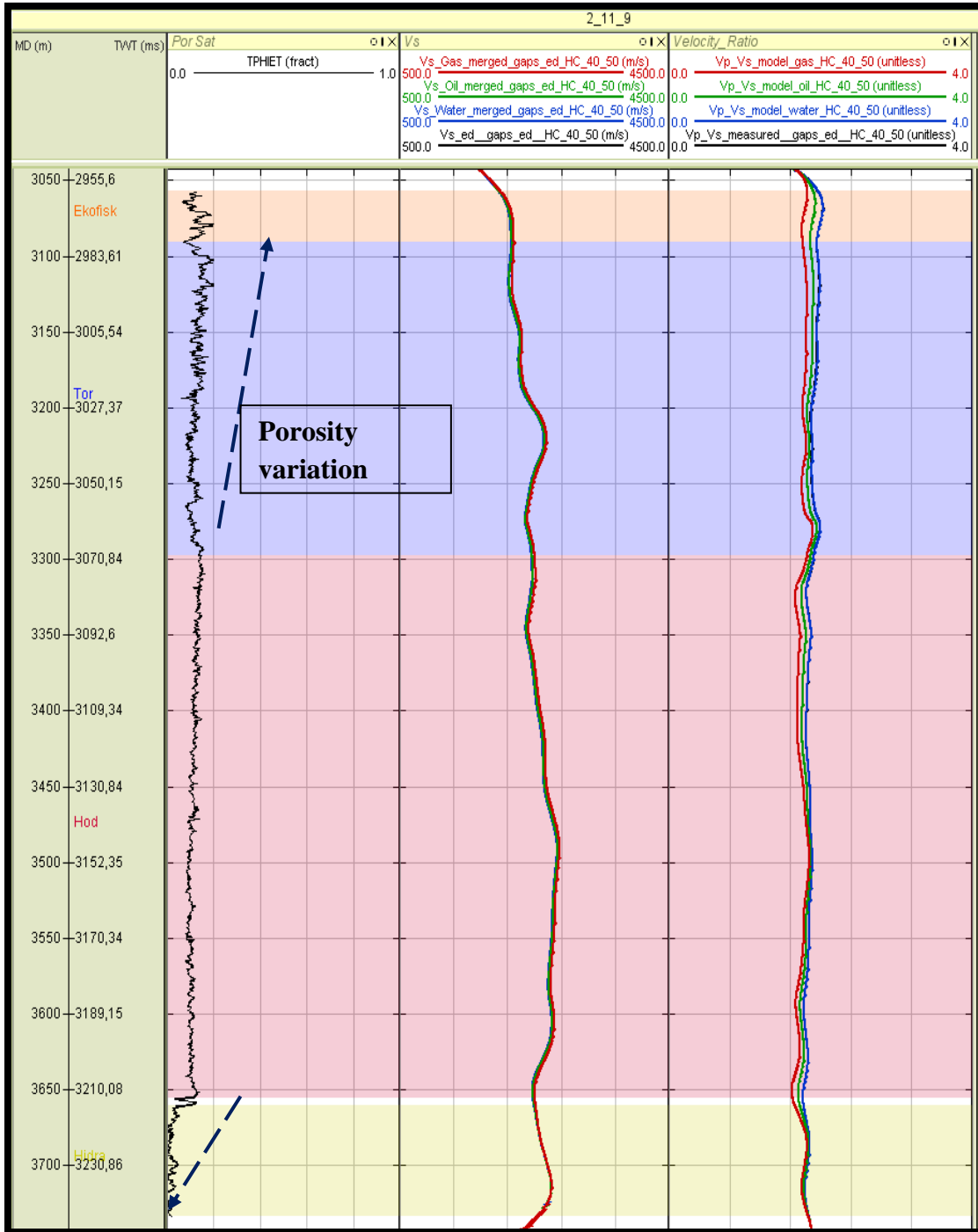


Figure 36: Three different fluids saturated filter logs (Well 2/11-9), oil (green), gas (red) and water (blue) saturation.

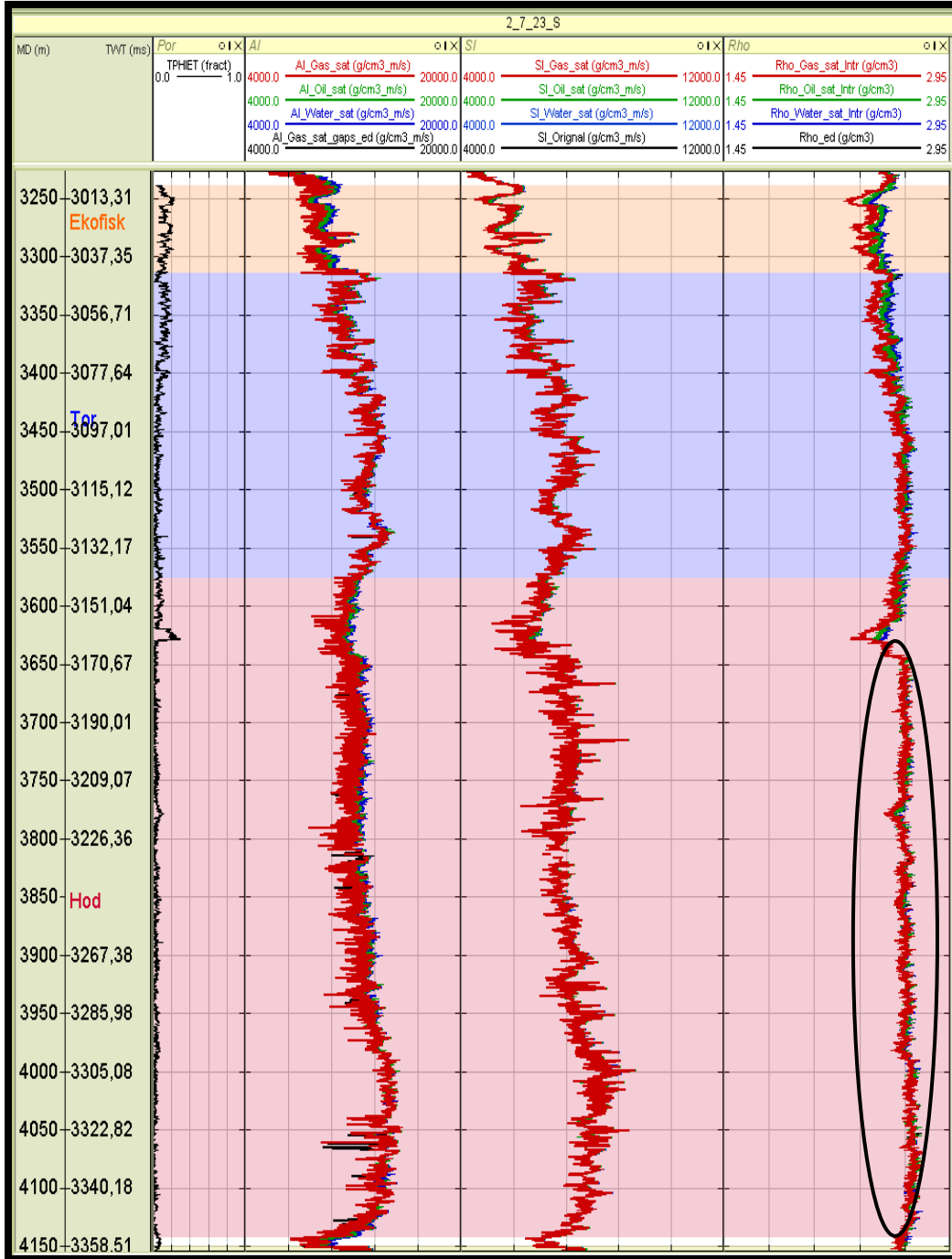


Figure 37: AI and SI in three different case of fluid saturation (well 2/7-23 S), oil (green), gas (red) and water (blue) saturation.

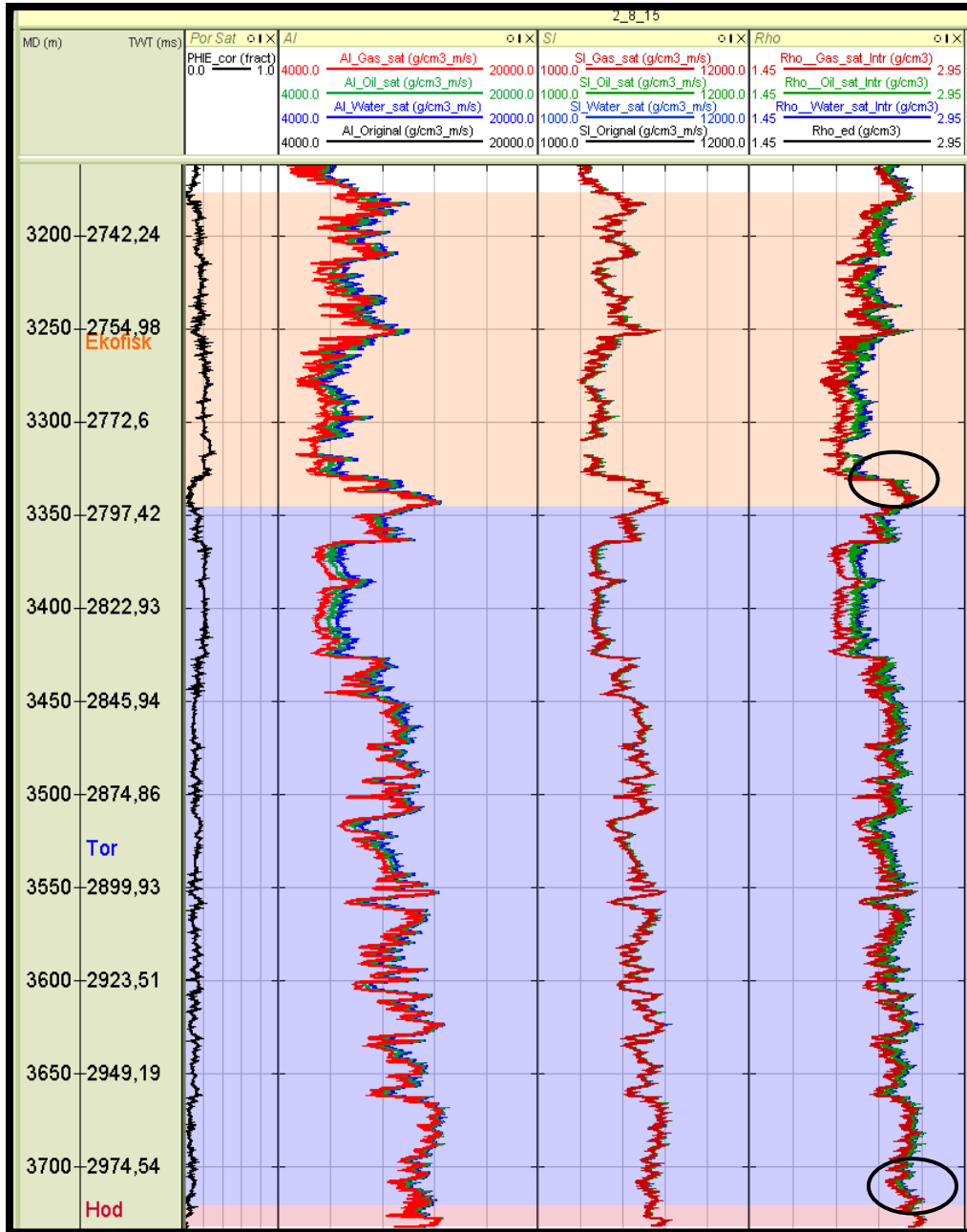


Figure 38: AI and SI in three different case of fluid saturation (well 2/8-15), oil (green), gas (red) and water (blue) saturation.

Comparison between acoustic and shear impedance in three scenario reveals that pores filled with fluids do not have any inspirational influence on the shear impedance logs (see figure 37, 38 &39). While acoustic impedance shows some informative variation in case of pores filled with different fluids. Variation in porosity of chalk was observed. Some place it was high at top and



decrease with depth (Figure: 34) while chalk of Hydra Formation had very low porosity in all wells. Well density in case of different kind of fluid saturation was showing variation except in some area there was no variation (Figures 37-39). There could be uncertainties which need to re check and more calibration.

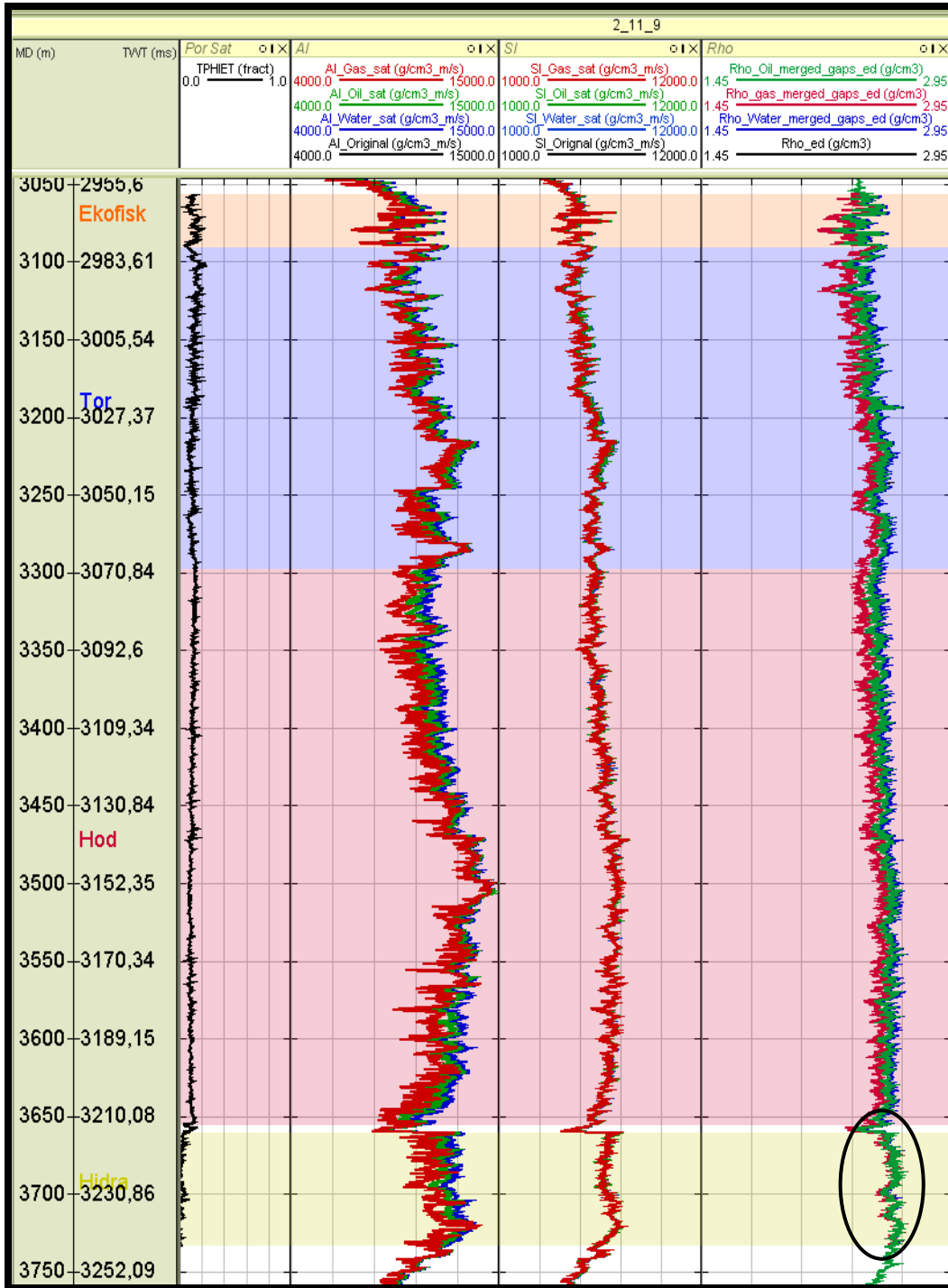


Figure 39: AI and SI in three different case of fluid saturation (well 2/11-9), oil (green), gas (red) and water (blue) saturation.

Seismic gathers were generated to understand the AVO effect in case of chalk formations saturated by water, oil and gas fluids. Seismic gathers were generated in Figure 40 to see the AVO effect in case of Chalk saturated by water. Top of Ekofisk the amplitude was sharp and

little bit increasing (negligible) with offset while in oil saturated case (Figure 41) this effect is more prominent similar effect can be observe in gas saturated case in Figure 42.

Meanwhile strange things were also happening with amplitude of seismic gather in the Chalk intervals which can be seen in figures (40-42) marked by black squares. They were showing variation in amplitude also with change of fluid type saturation but porosity factor was also noted because at these point porosity was low which means that low porous chalk saturated with fluid can be distinguishable on seismic.

The bottom of fluids saturated chalk behavior is clearly visible in figures (40-42). At zero offset it has high contrast which was diminishing with increase in offset but in three scenarios case it is bit hard say about the difference between types of fluids present in Chalk.

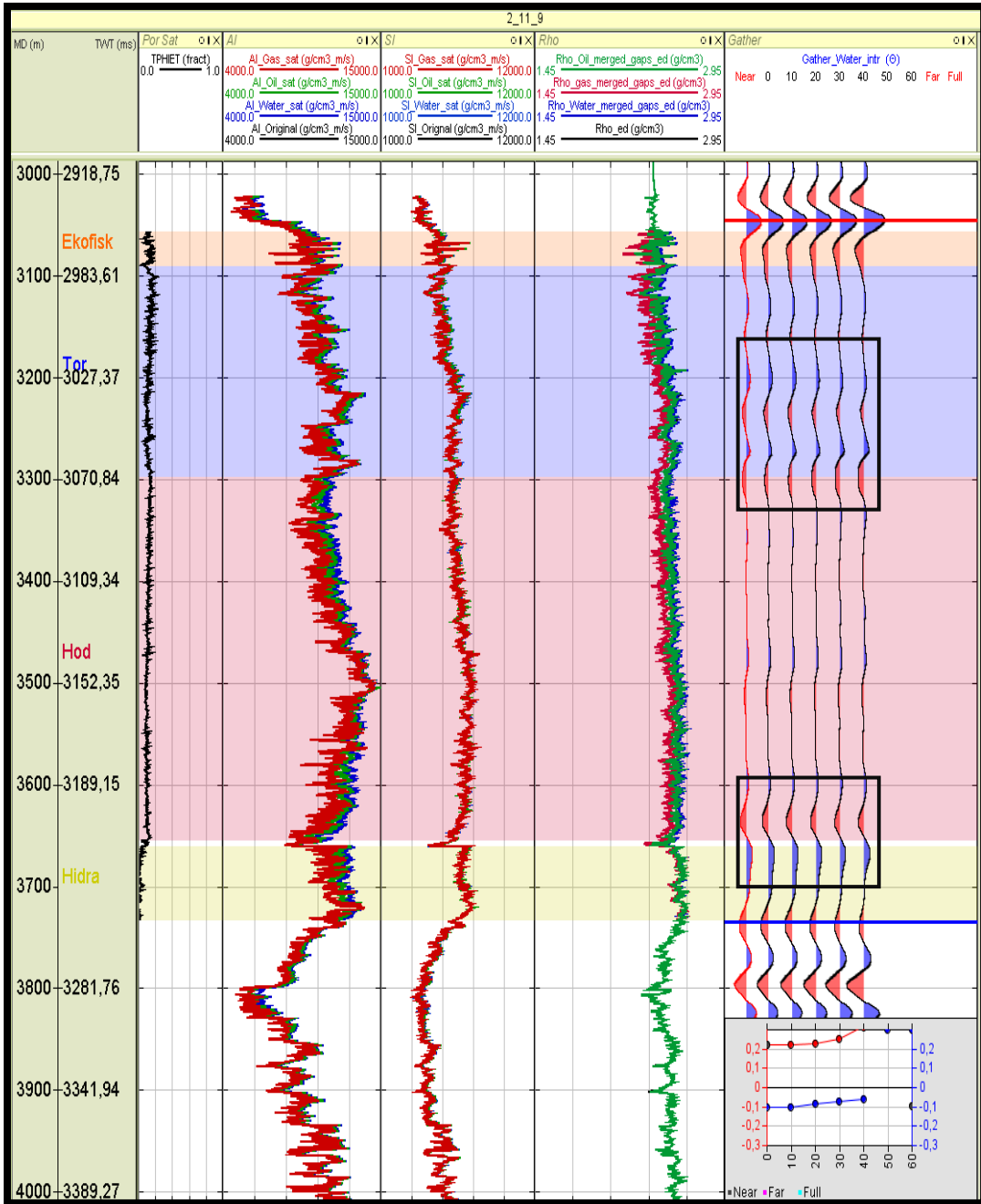


Figure 40: Water saturated AVO effect of seismic gathers (well 2/11-9).

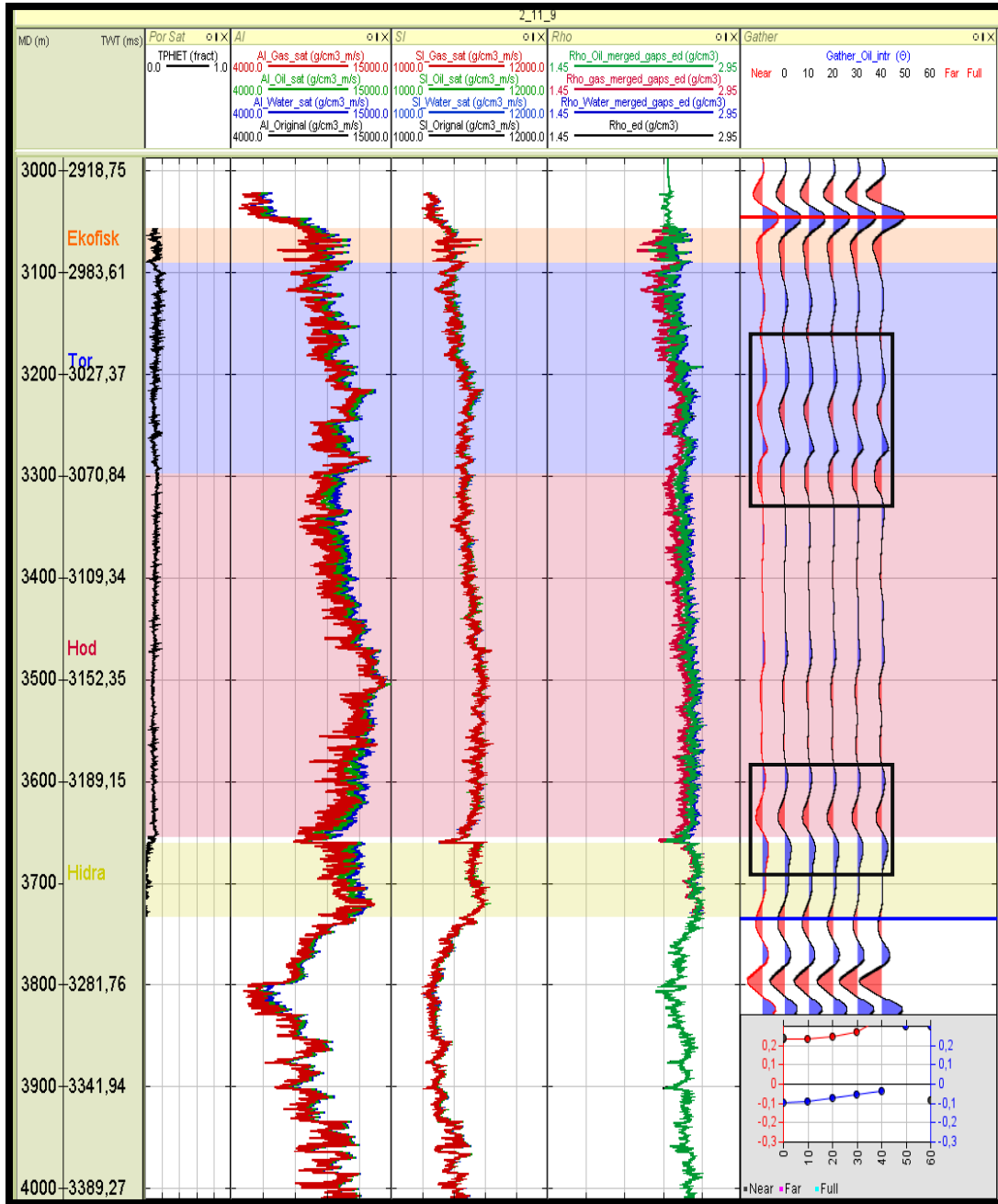


Figure 41: Oil saturated AVO effect of seismic gathers (well 2/11-9).

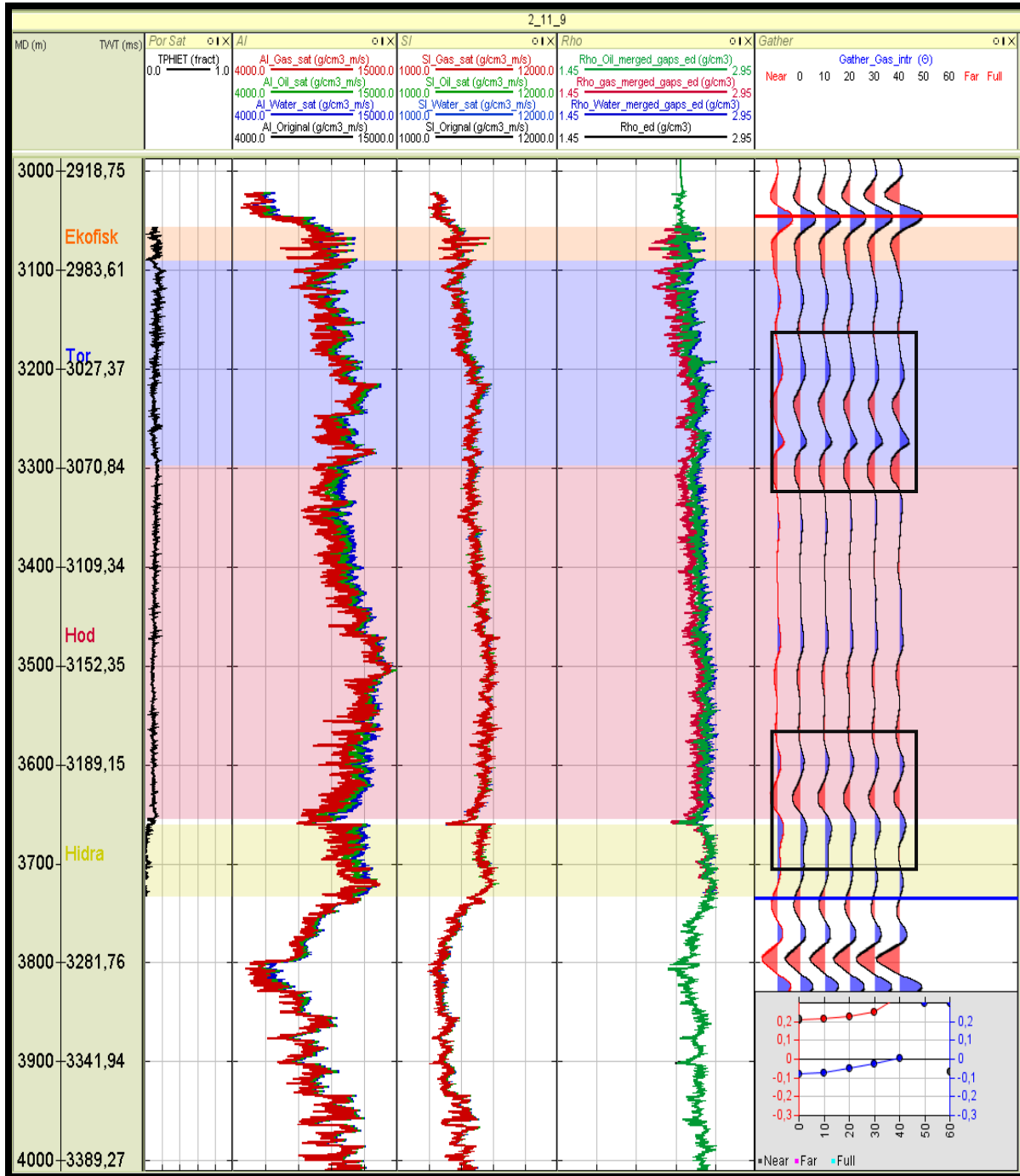


Figure 42: Gas saturated AVO effect of seismic gathers (well 2/11-9).

## **6 Cross Plots for Reservoir Analysis**

### **6.1 Introduction**

The elastic properties such as velocity, density, impedance and Vp/Vs ratio take an important role in reservoir characterization because they are related to the reservoir properties (Xin-Gang & De-Hua Han, 2009). Characterizing the elastic properties of reservoir very closely cross plots approach was used. The idea behind this was to generate the cross plots of modeled and measured logs especially acoustic Impedance, shear Impedance and VpVs ratios and logs were filter in seismic domain.

### **6.2 Shear versus Acoustic Impedance**

Cross plots between Shear (SI) and Acoustic (AI) Impedance measured and modeled logs were generated. These logs were water, oil and gas saturated. Logs were also filtered in seismic domain (TWT domain).

Figures 43-45 are cross plots of water, oil and gas saturated modeled shear and acoustic impedance logs which is color coded with effective porosity. All this data is for characterizing the chalk of Ekofisk, Tor, Hod and Hidra. AI and Si ranges were highlighted by dote light blues for values which were coded with high porosity values (Figure 43-47).

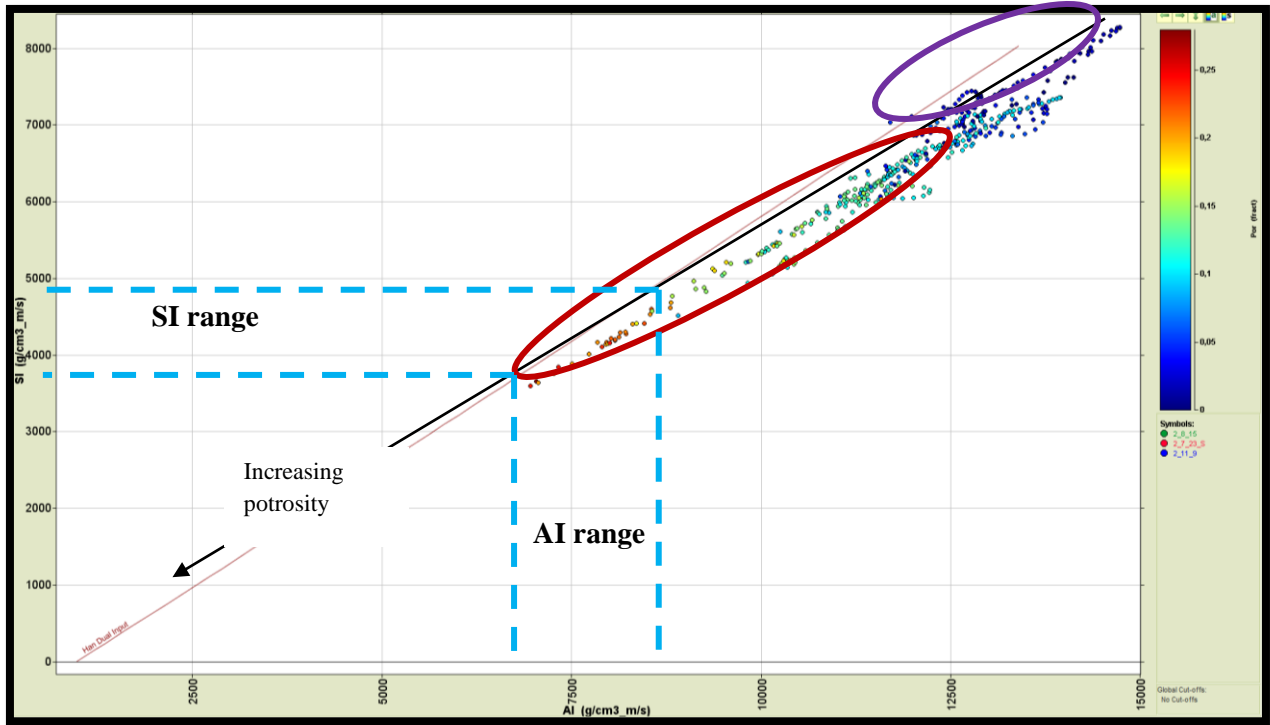


Figure 43: Cross plots between water saturated AI and SI filtered logs colored coded with effective porosity.

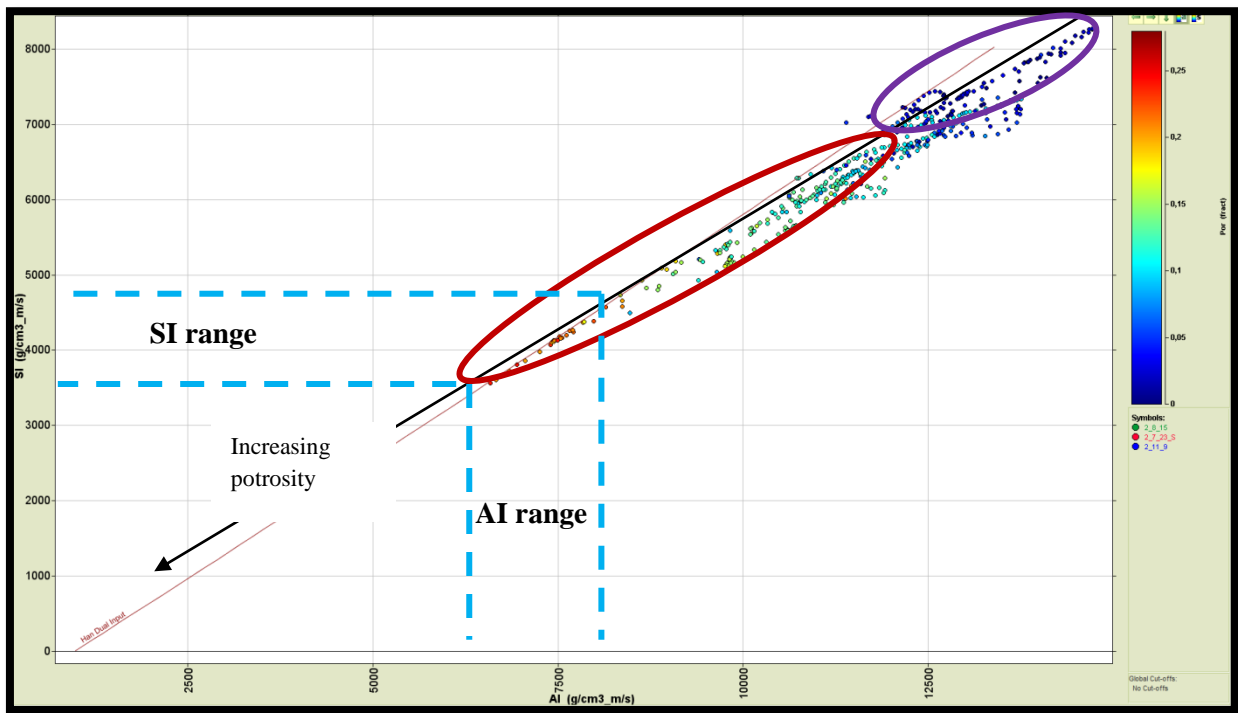


Figure 44: Cross plots between Oil saturated AI and SI filtered logs color coded with effective porosity.



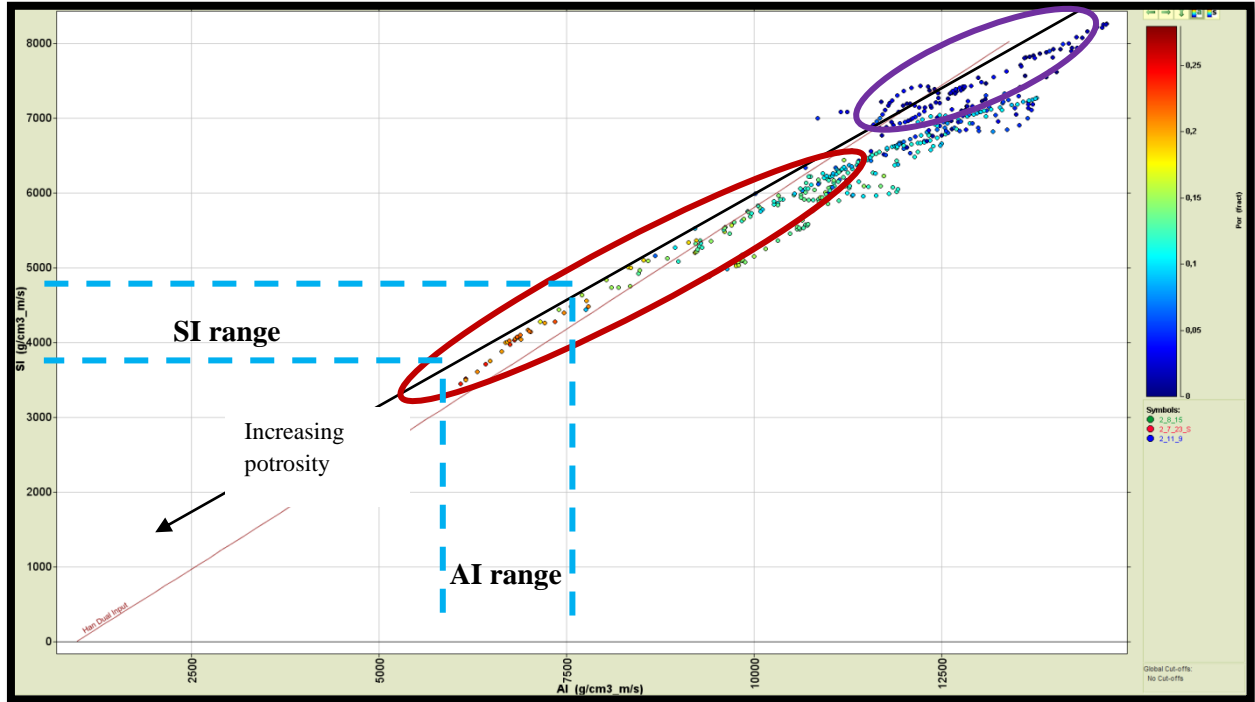


Figure 45: Cross plots between Gas saturated AI and SI filtered logs color coded with effective porosity.

X-axis is representing Acoustic Impedance of different fluid saturated modeled logs while y-axis is of Shear Impedance of modeled fluid saturated logs. Color bar is representing that point in cross plots are coded with effective porosity. Black arrow is representing the increasing trend of porosity.

Effective porosity is dividing Chalk into two different trends. Dark blue coded data is showing that porosity of chalk is very low with high AI and SI values and don't have fluid effect. Similarly for oil and gas saturated plots (Figure: 43-45).

While the chalk with medium to high porosity values is easily visible on the cross plots which is highlighted by red polygon. Porosity saturated with different fluid is showing their variant impact on the acoustic and shear impedance. Red points are very high porosity chawks saturated with different fluids. In figures (43-45) light blue color dotted lines are representing the range of shear and acoustic impedance. It was observed that pore fluid have great influence on acoustic impedance (Figure: 4-45).

Acoustic impedance is decreasing with change of type fluid (Figure: 43-45) while shear impedance is not showing any influence.

Same approach was adopted for HC saturated and Water Saturated wells to find out their trend by using measured logs to see the level of effectiveness of the modeled cross plot.

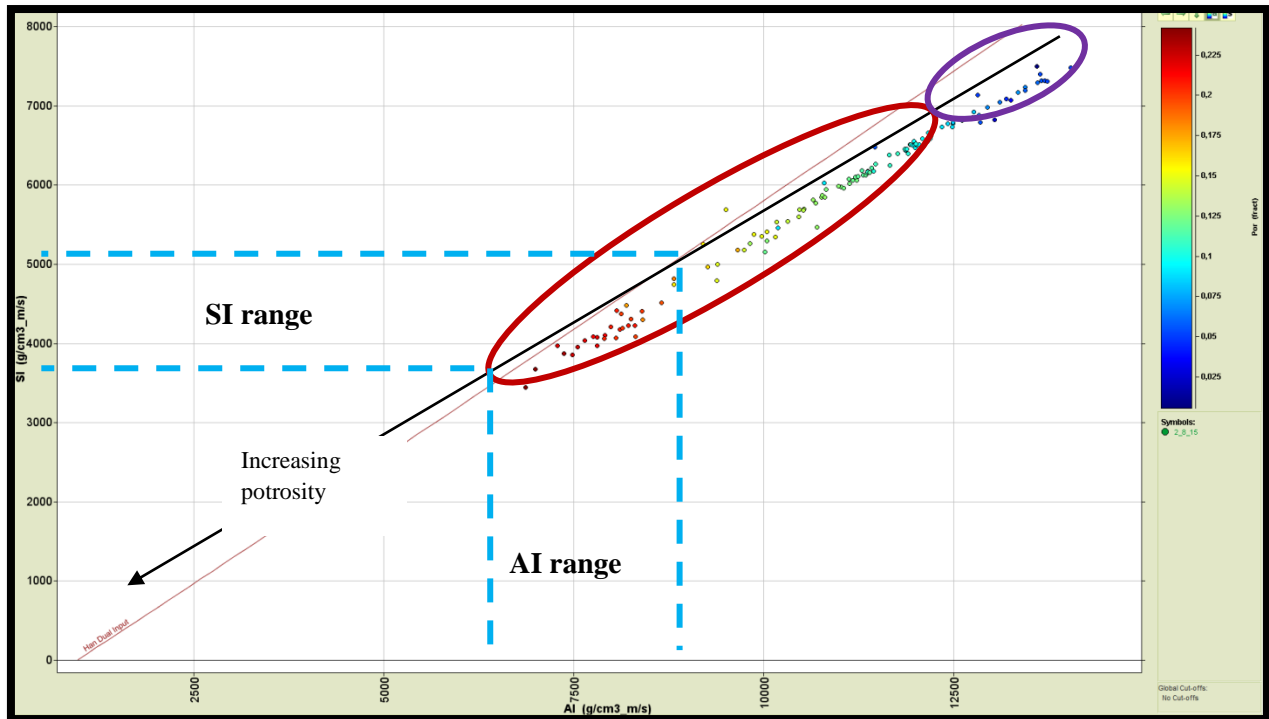


Figure 46: Measure acoustic and shear impedance cross plot using well 2/8-15.

Figure 46 is cross plot between acoustic (x-axis) and shear (y-axis) using HC saturated logs of well 2/8-15 and also color coded with effective porosity. Low porosity points are in blue polygon with high AI and SI values while Low SI and AI points are in red polygon representing the high porosity and saturated with water. AI and SI impedance ranges of complete water saturated rocks are bounded in dotted light blue color lines.

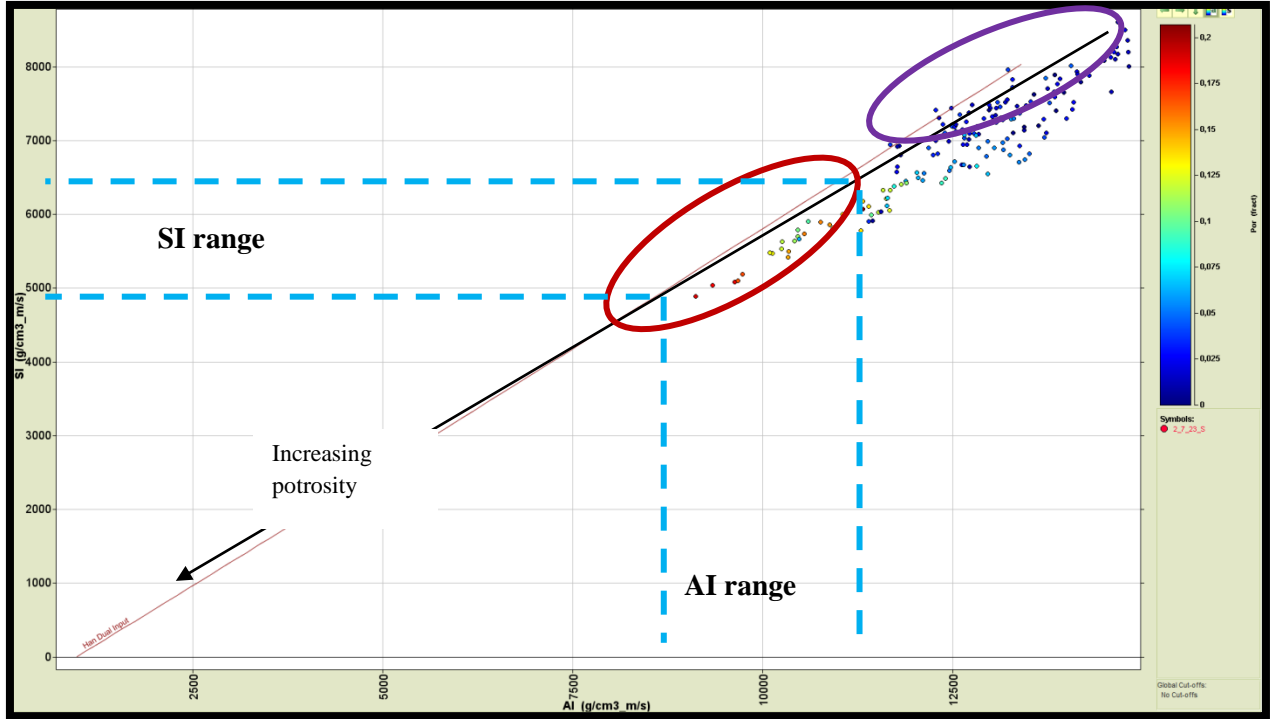


Figure 47: Measure acoustic and shear impedance cross plot using well 2/7-23S.

Measured Filter logs of well 2/7-23S were used to see the response of shear and acoustic impedance in case of oil saturated logs. Here shear and acoustic impedance of HC saturated porous (high) chalk was high (Figure 47).

There were some uncertain points which were showing dual trend for example low and high porosity values were at same acoustic and shear impedance values.

### 6.3 VpVs versus Acoustic Impedance

VpVs cross plot was generated to see the behavior of porosity and fluid substituted in pores of reservoir. Measured cross plots were generated by substituting different fluid to characterize the reservoir more confidently (see figure 48-50).

Figures 48-50 is about to characterize the reservoir properties in case of pore saturated with water, oil and gas. Increment in porosity trend can be seen in figures and the variation in VpVs due to change in pore fluid is clearly visible or prominent than Acoustic Impedance. Lithology

and fluid can also clearly delineate if same approach will be adopted for cross plot the elastic parameters coded with GR log.

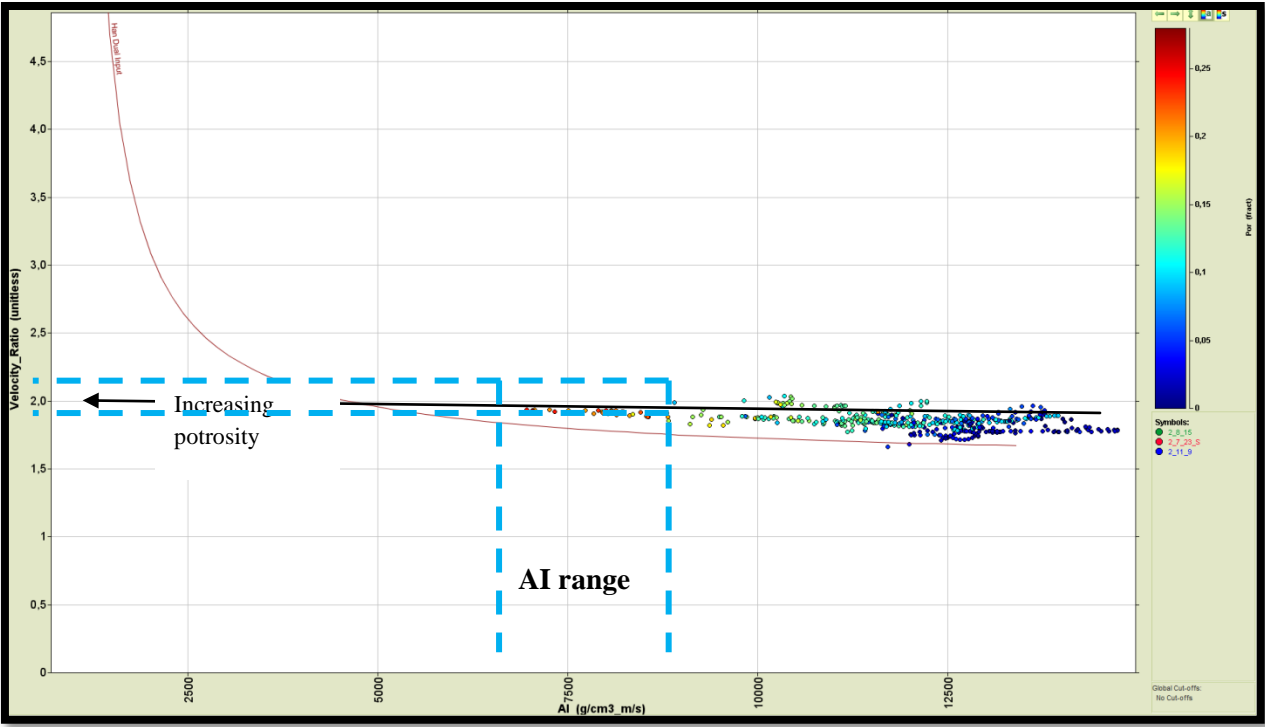


Figure 48: VpVs versus AI (acoustic Impedance) cross plot of water saturated modeled logs.

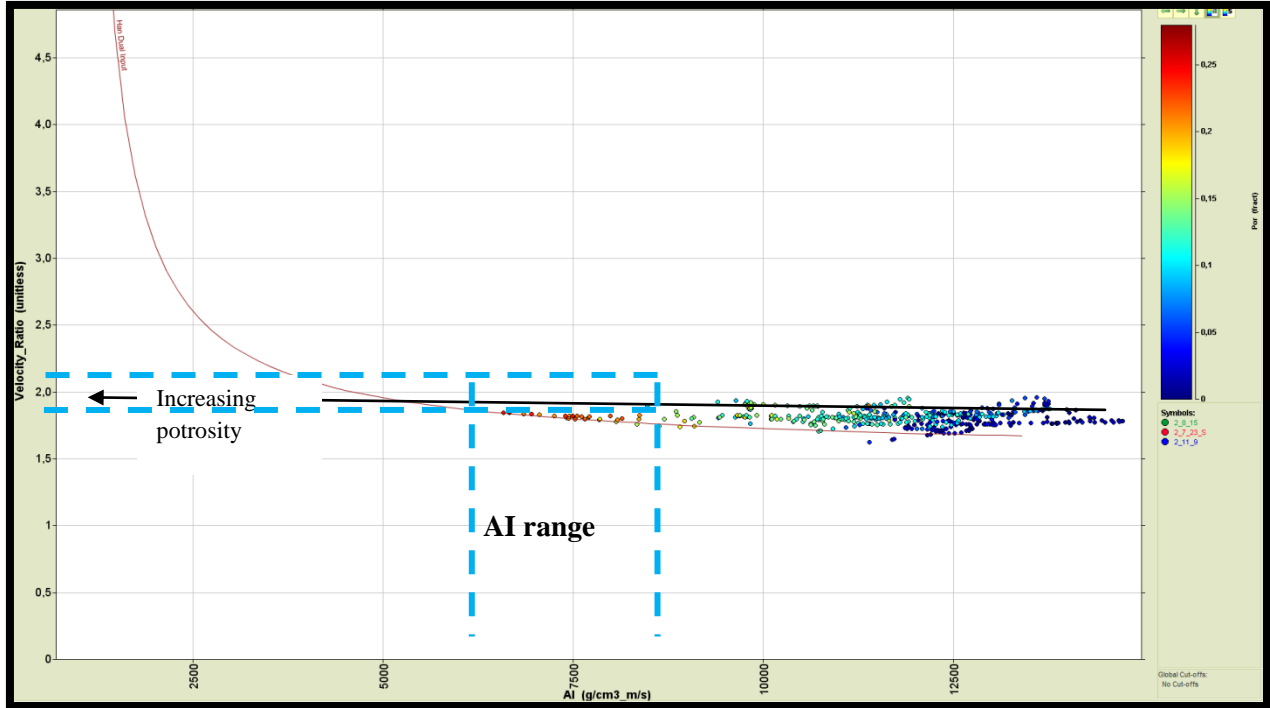


Figure 49: VpVs versus AI (acoustic Impedance) cross plot of oil saturated modeled logs.

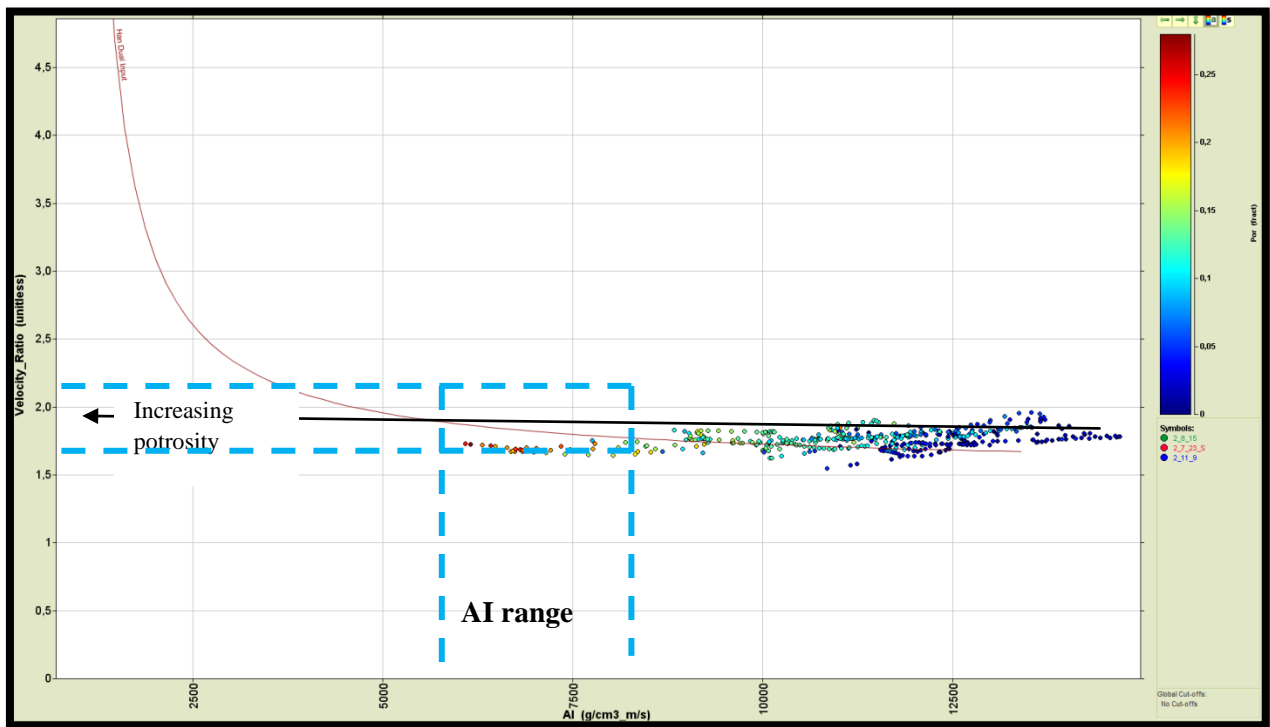


Figure 50: VpVs versus AI (acoustic Impedance) cross plot of gas saturated modeled logs.

## **7 Conclusions & Recommendations**

### **7.1 Conclusions**

After running the Petro physical and Rock physical workflow, it is concluded that cross plot of elastic parameters are helpful to delineate the lithology and fluid and their effects. It is possible to predict the shear velocity and fluid content of that virgin area using the surrounding wells information (Figure 26-27). It is also helpful to predict the pore fluid effect on seismic data from zero to far offsets (Figure 40-42). This approach can be useful for seismic interpreter to identify the fluid saturated reservoirs on seismic more confidently.

### **7.2 Recommendations**

As previous theories and models are for Sand lithologies but our model is of Chalk. On the basis of data provided for this task and limited availability of time it will be risky to give any big statement. On the basis of work experience on this project I will like to recommend that to make better model for Chalk it would be good to do detail petrophysical studies of area using core data and increasing the number of wells. Because for this task three well were used and quality of wells were not good specially shear sonic data. Core data and well reports were also not available. For investigating the effect of different fluids on seismic gathers with respect to offset increment check shot were used to make synthetic gathers. The Quality of check shots was not of good quality and they were very old. There was delay in getting new and better check shots and also core data. That's why limited data was used for preparation of feasibility report for PL 616. But Rock physical analysis, Seismic Inversion and AVO analysis can be useful to characterize chalk reservoir properly and can be helpful to delineate fluid related bright spot on Seismic data.

## 8 References

- Buland, A. (2012). Seismic Amplitude Analysis and Inversion. In A. Buland, Compendium GEO 610 (pp.49-50). Stavanger.
- Buland, A. (2012). Seismic Amplitude Analysis And Inversion. In A. Buland, Compendium Geo 610 (pp. 10-12). Stavanger.
- Buland, A. (October 7, 2012). Seismic Amplitude Analysis And Inversion. Stavanger.
- Buland, A. (2012). Seismic amplitude analysis and Seismic Inversion. In A. Buland, compendium Geo 610 (pp. 54-55). Stavanger.
- Buland, A. (2012). Seismic Amplitude Analysis And Seismic Inversion. In A. Buland, Compendium GEO610 (pp. 52-53). Stavanger.
- Dewar, J. (2001). Rock physics for the rest of us- An informal discussion. CSEG recoder , 42-49.
- Evans, D., Graham, C., Armur, A., & Bathrust, P. (2003). Petroleum Geology of Central and Northren North Sea. London: Geological Society of London.
- Gibbs, J. P., Barcelona, M. J., D, J., & Lefavivre, M. H. (1984). Effective Porosity Of Geological Material. Illinois: Department of Energy and Natural Resources.
- Google. (2013). Retrieved May 22, 2013, from Schlumberger:  
<http://www.glossary.oilfield.slb.com/en/Terms.aspx?LookIn=term%20name&filter=effective%20porosity>
- Goolge. (n.d.). Retrieved May 12, 2013, from image.google.com:  
<http://www.kgs.ku.edu/HighPlains/atlas/porfig.gif>
- Norwegian Petrolwum Directorate. (n.d.). Retrieved May 15, 2013, from <http://npd.no/en/>
- Per Avseth, Tapan Mukerji, & Gary Mavko. (2005). Quantitative Seismic Interpretation. United Kingdom: Cambridge University Press.
- Rider, M., & Kennedy, M. (2011). The Geological Interpretation of Well Logs. Glasgow: Rider-French Consulting Ltd.
- Xin-Gang, & De-Hua Han. (2009). Lithology and fluid differentiation using a rock physics template. The Leading Edge , 60-65.
- Buland, A. (2012). Seismic Amplitude Analysis And Inversion. In A. Buland, Compendium Geo 610 (pp. 113-114). Stavanger.

